4. Lathrop JT, Timko MP. Regulation by heme of mitochondrial protein transport through a conserved amino acid motif. Science. 1993;259: 522–525.
5. Munakata H, Sun JY, Yoshida K, et al. Role of the heme regulatory motif in the heme-mediated inhibition of mitochondrial import of 5-aminolevulinate synthase. J Biochem. 2004;136:233–238.
6. Dailey TA, Woodruff JH, Dailey HA. Examination of mitochondrial protein targeting of haem synthetic enzymes: in vivo identification of three functional haem-responsive motifs in 5-aminolaevulinate synthase. Biochem J. 2005;386:381–386.
7. Munakata H, Yamagami T, Nagai T, Yamamoto M, Hayashi N. Purification and structure of rat erythroid-specific delta-aminolevulinate synthase. J Biochem. 1993;114:103–111.
8. Cox TC, Bawden MJ, Abraham NG, et al. Erythroid 5-aminolevulinate synthase is located on the X chromosome. Am J Hum Genet. 1990;46:107–111.
9. Cox TC, Bottomley SS, Wiley JS, Bawden MJ, Matthews CS, May BK. X-linked pyridoxine-responsive sideroblastic anemia due to a Thr388-to-Ser substitution in erythroid 5-aminolevulinate synthase. N Engl J Med. 1994;330:675–679.
10. Cotter PD, Baumann M, Bishop DF. Enzymatic defect in "X-linked" sideroblastic anemia: molecular evidence for erythroid delta-aminolevulinate synthase deficiency. Proc Natl Acad Sci U S A. 1992;89:4028–4032.
11. Whatley SD, Ducamp S, Gouya L, et al. C-terminal deletions in the ALAS2 gene lead to gain of function and cause X-linked dominant protoporphyria without anemia or iron overload. Am J Hum Genet. 2008;83:408–414.
12. Bottomley SS. Sideroblastic anemias. In: Greer JP, Foerster J, Rogers GM, et al., eds. Wintrobe's Clinical Hematology. 12th ed. Philadelphia/London: Wolters Kluwer Health/Lippincott Williams & Wilkins; 2009. p. 835–856.
13. Harigae H, Furuyama K. Hereditary sideroblastic anemia: pathophysiology and gene mutations. Int J Hematol. 2010;92:425–431.
14. Ducamp S, Kannengiesser C, Touati M, et al. Sideroblastic anemia: molecular analysis of the ALAS2 gene in a series of 29 probands and functional studies of 10 missense mutations. Hum Mutat. 2011; 32:590–597.
15. Harigae H, Furuyama K, Kimura A, et al. A novel mutation of the erythroid-specific delta-aminolaevulinate synthase gene in a patient with X-linked sideroblastic anaemia. Br J Haematol. 1999;106:175–177.
16. Cazzola M, May A, Bergamaschi G, Cerani P, Ferrillo S, Bishop DF. Absent phenotypic expression of X-linked sideroblastic anemia in one of 2 brothers with a novel ALAS2 mutation. Blood. 2002;100: 4236–4238.
17. Astner I, Schulze JO, van den Heuvel J, Jahn D, Schubert WD, Heinz DW. Crystal structure of 5-aminolevulinate synthase, the first enzyme of heme biosynthesis, and its link to XLSA in humans. EMBO J. 2005; 24:3166–3177.
18. To-Figueras J, Ducamp S, Clayton J, et al. ALAS2 acts as a modifier gene in patients with congenital erythropoietic porphyria. Blood. 2011;118:1443–1451.
19. Sambrook J, Russell DW. Molecular Cloning: A Laboratory Manual. 3rd ed. Cold Spring Harbor, NY: Cold Spring Harbor Laboratory Press; 2001.
20. Furuyama K, Fujita H, Nagai T, et al. Pyridoxine refractory X-linked sideroblastic anemia caused by a point mutation in the erythroid 5-aminolevulinate synthase gene. Blood. 1997;90:822–830.
21. Furuyama K, Harigae H, Heller T, et al. Arg452 substitution of the erythroid-specific 5-aminolaevulinate synthase, a hot spot mutation in X-linked sideroblastic anaemia, does not itself affect enzyme activity. Eur J Haematol. 2006;76:33–41.
22. Furuyama K, Sassa S. Interaction between succinyl CoA synthetase and the heme-biosynthetic enzyme ALAS-E is disrupted in sideroblastic anemia. J Clin Invest. 2000;105:757–764.
23. Kaneko K, Furuyama K, Aburatani H, Shibahara S. Hypoxia induces erythroid-specific 5-aminolevulinate synthase expression in human erythroid cells through transforming growth factor-beta signaling. FEBS J. 2009;276:1370–1382.
24. Guernsey DL, Jiang H, Campagna DR, et al. Mutations in mitochondrial carrier family gene SLC25A38 cause nonsyndromic autosomal recessive congenital sideroblastic anemia. Nat Genet. 2009;41:651–653.
25. Ye H, Jeong SY, Ghosh MC, et al. Glutaredoxin 5 deficiency causes sideroblastic anemia by specifically impairing heme biosynthesis and depleting cytosolic iron in human erythroblasts. J Clin Invest. 2010;120:1749–1761.
26. Allikmets R, Raskind WH, Hutchinson A, Schueck ND, Dean M, Koeller DM. Mutation of a putative mitochondrial iron transporter gene (ABC7) in X-linked sideroblastic anemia and ataxia (XLSA/A). Hum Mol Genet. 1999;8:743–749.
27. Bykhovskaya Y, Casas K, Mengesha E, Inbal A, Fischel-Ghodsian N. Missense mutation in pseudouridine synthase 1 (PUS1) causes mitochondrial myopathy and sideroblastic anemia (MLASA). Am J Hum Genet. 2004;74:1303–1308.
28. Ricketts CJ, Minton JA, Samuel J, et al. Thiamine-responsive megaloblastic anaemia syndrome: long-term follow-up and mutation analysis of seven families. Acta Paediatr. 2006;95:99–104.
29. Rotig A, Colonna M, Bonnefont JP, et al. Mitochondrial DNA deletion in Pearson's marrow/pancreas syndrome. Lancet. 1989;1:902–903.
30. Bergmann AK, Campagna DR, McLoughlin EM, et al. Systematic molecular genetic analysis of congenital sideroblastic anemia: evidence for genetic heterogeneity and identification of novel mutations. Pediatr Blood Cancer. 2010;54:273–278.
31. Cotter PD, Rucknagel DL, Bishop DF. X-linked sideroblastic anemia: identification of the mutation in the erythroid-specific delta-aminolevulinate synthase gene (ALAS2) in the original family described by Cooley. Blood. 1994;84:3915–3924.
32. Cotter PD, May A, Fitzsimons EJ, et al. Late-onset X-linked sideroblastic anemia. Missense mutations in the erythroid delta-aminolevulinate synthase (ALAS2) gene in two pyridoxine-responsive patients initially diagnosed with acquired refractory anemia and ringed sideroblasts. J Clin Invest. 1995;96:2090–2096.
33. Prades E, Chambon C, Dailey TA, Dailey HA, Briere J, Grandchamp B. A new mutation of the ALAS2 gene in a large family with X-linked sideroblastic anemia. Hum Genet. 1995;95:424–428.
34. Furuyama K, Uno R, Urabe A, et al. R411C mutation of the ALAS2 gene encodes a pyridoxine-responsive enzyme with low activity. Br J Haematol. 1998;103:839–841.
35. Harigae H, Furuyama K, Kudo K, et al. A novel mutation of the erythroid-specific delta-Aminolevulinate synthase gene in a patient with non-inherited pyridoxine-responsive sideroblastic anemia. Am J Hematol. 1999;62:112–114.
36. Furuyama K, Harigae H, Kinoshita C, et al. Late-onset X-linked sideroblastic anemia following hemodialysis. Blood. 2003;101: 4623–4624.
37. Ferreira GC, Neame PJ, Dailey HA. Heme biosynthesis in mammalian systems: evidence of a Schiff base linkage between the pyridoxal 5'-phosphate cofactor and a lysine residue in 5-aminolevulinate synthase. Protein Sci. 1993;2:1959–1965.
38. Gong J, Ferreira GC. Aminolevulinate synthase: functionally important residues at a glycine loop, a putative pyridoxal phosphate cofactor-binding site. Biochemistry. 1995;34:1678–1685.
39. Tan D, Ferreira GC. Active site of 5-aminolevulinate synthase resides at the subunit interface. Evidence from in vivo heterodimer formation. Biochemistry. 1996;35:8934–8941.
40. Gong J, Hunter GA, Ferreira GC. Aspartate-279 in aminolevulinate synthase affects enzyme catalysis through enhancing the function of the pyridoxal 5'-phosphate cofactor. Biochemistry. 1998;37:3509–3517.
41. Tan D, Barber MJ, Ferreira GC. The role of tyrosine 121 in cofactor binding of 5-aminolevulinate synthase. Protein Sci. 1998;7:1208–1213.

42. Tan D, Harrison T, Hunter GA, Ferreira GC. Role of arginine 439 in substrate binding of 5-aminolevulinate synthase. Biochemistry. 1998; 37:1478–1484.
43. Turbeville TD, Zhang J, Hunter GA, Ferreira GC. Histidine 282 in 5-aminolevulinate synthase affects substrate binding and catalysis. Biochemistry. 2007;46:5972–5981.
44. Lendrihas T, Zhang J, Hunter GA, Ferreira GC. Arg-85 and Thr-430 in murine 5-aminolevulinate synthase coordinate acyl-CoA-binding and contribute to substrate specificity. Protein Sci. 2009;18:1847–1859.
45. Lendrihas T, Hunter GA, Ferreira GC. Serine 254 enhances an induced fit mechanism in murine 5-aminolevulinate synthase. J Biol Chem. 2010;285:3351–3359.
46. Lendrihas T, Hunter GA, Ferreira GC. Targeting the active site gate to yield hyperactive variants of 5-aminolevulinate synthase. J Biol Chem. 2010;285:13704–13711.
47. Zhang J, Ferreira GC. Transient state kinetic investigation of 5-aminolevulinate synthase reaction mechanism. J Biol Chem. 2002;277: 44660–44669.

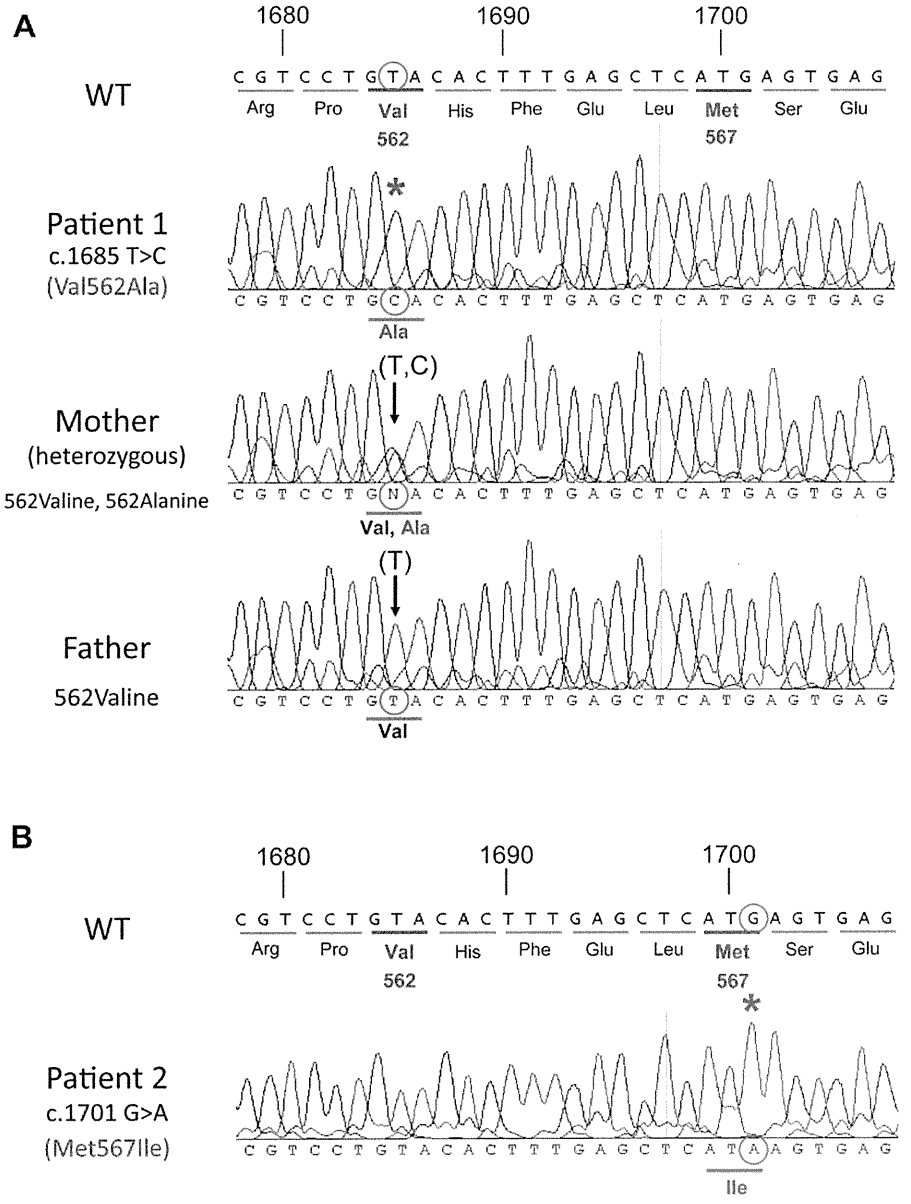

Supplementary Figure E1. Direct sequencing of 11th exon of ALAS2 gene in patients with sideroblastic anemia. Exon 11 of ALAS2 gene from each proband was amplified by PCR, and the amplicon was sequenced directly. Numbers shown at top indicate the positions of cDNA sequence, which is started from the first nucleotide of the ATG-translation initiation codon. Second and third lines indicate wild-type DNA sequence and amino acid sequence, respectively. Identified mutations are indicated with asterisks, and the expected amino acid substitution is shown under each mutation. (**A**) The c.1685T>C mutation of ALAS2 gene in case 1. The heterozygous condition of proband's mother and the wild-type allele of proband's father are shown. (**B**) The c.1701G>A mutation of ALAS2 gene in case 2.

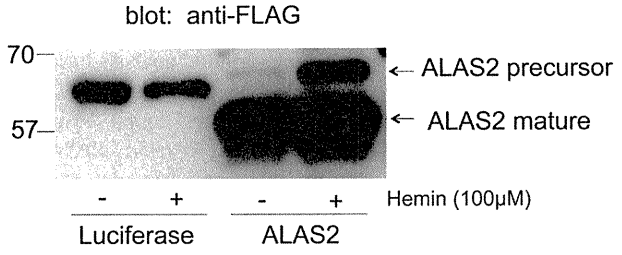

Supplementary Figure E2. Transient expression of FLAG-ALAS2 and FLAG-Luciferase in HeLa cells. HeLa human cervical cancer cells were transfected with FLAG-ALAS2 or FLAG-luciferase expression vector, then treated with 100 μM hemin. Cell lysates were subjected to the Western blot analysis with anti-FLAG antibody. Shown are the representative data.

Extensive gene deletions in Japanese patients with Diamond-Blackfan anemia

Madoka Kuramitsu,[1] Aiko Sato-Otsubo,[2] Tomohiro Morio,[3] Masatoshi Takagi,[3] Tsutomu Toki,[4] Kiminori Terui,[4] RuNan Wang,[4] Hitoshi Kanno,[5] Shouichi Ohga,[6] Akira Ohara,[7] Seiji Kojima,[8] Toshiyuki Kitoh,[9] Kumiko Goi,[10] Kazuko Kudo,[11] Tadashi Matsubayashi,[12] Nobuo Mizue,[13] Michio Ozeki,[14] Atsuko Masumi,[1] Haruka Momose,[1] Kazuya Takizawa,[1] Takuo Mizukami,[1] Kazunari Yamaguchi,[1] Seishi Ogawa,[2] Etsuro Ito,[4] and Isao Hamaguchi[1]

[1]Department of Safety Research on Blood and Biological Products, National Institute of Infectious Diseases, Tokyo, Japan; [2]Cancer Genomics Project, Graduate School of Medicine, The University of Tokyo, Tokyo, Japan; [3]Department of Pediatrics and Developmental Biology, Graduate School of Medicine, Tokyo Medical and Dental University, Bunkyo-ku, Tokyo, Japan; [4]Department of Pediatrics, Hirosaki University Graduate School of Medicine, Hirosaki, Japan; [5]Department of Transfusion Medicine and Cell Processing, Tokyo Women's Medical University, Tokyo, Japan; [6]Department of Pediatrics, Graduate School of Medical Sciences, Kyushu University, Fukuoka, Japan; [7]First Department of Pediatrics, Toho University School of Medicine, Tokyo, Japan; [8]Department of Pediatrics, Nagoya University Graduate School of Medicine, Nagoya, Japan; [9]Department of Hematology/Oncology, Shiga Medical Center for Children, Shiga, Japan; [10]Department of Pediatrics, School of Medicine, University of Yamanashi, Yamanashi, Japan; [11]Division of Hematology and Oncology, Shizuoka Children's Hospital, Shizuoka, Japan; [12]Department of Pediatrics, Seirei Hamamatsu General Hospital, Shizuoka, Japan; [13]Department of Pediatrics, Kushiro City General Hospital, Hokkaido, Japan; and [14]Department of Pediatrics, Graduate School of Medicine, Gifu University, Gifu, Japan

Fifty percent of Diamond-Blackfan anemia (DBA) patients possess mutations in genes coding for ribosomal proteins (RPs). To identify new mutations, we investigated large deletions in the RP genes *RPL5*, *RPL11*, *RPL35A*, *RPS7*, *RPS10*, *RPS17*, *RPS19*, *RPS24*, and *RPS26*. We developed an easy method based on quantitative-PCR in which the threshold cycle correlates to gene copy number. Using this approach, we were able to diagnose 7 of 27 Japanese patients (25.9%) possessing mutations that were not detected by sequencing. Among these large deletions, similar results were obtained with 6 of 7 patients screened with a single nucleotide polymorphism array. We found an extensive intragenic deletion in *RPS19*, including exons 1-3. We also found 1 proband with an *RPL5* deletion, 1 patient with an *RPL35A* deletion, 3 with *RPS17* deletions, and 1 with an *RPS19* deletion. In particular, the large deletions in the *RPL5* and *RPS17* alleles are novel. All patients with a large deletion had a growth retardation phenotype. Our data suggest that large deletions in RP genes comprise a sizable fraction of DBA patients in Japan. In addition, our novel approach may become a useful tool for screening gene copy numbers of known DBA genes. (*Blood*. 2012;119(10): 2376-2384)

Introduction

Diamond-Blackfan anemia (DBA; MIN# 105650) is a rare congenital anemia that belongs to the inherited BM failure syndromes, generally presenting in the first year of life. Patients typically present with a decreased number of erythroid progenitors in their BM.[1] A main feature of the disease is red cell aplasia, but approximately half of patients show growth retardation and congenital malformations in the craniofacial, upper limb, cardiac, and urinary systems. Predisposition to cancer, in particular acute myeloid leukemia and osteogenic sarcoma, is also characteristic of the disease.[2]

Mutations in the *RPS19* gene were first reported in 25% of DBA patients by Draptchinskaia et al in 1999.[3] Since that initial finding, many genes that encode large (RPL) or small (RPS) ribosomal subunit proteins were found to be mutated in DBA patients, including *RPL5* (approximately 21%), *RPL11* (approximately 9.3%), *RPL35A* (3.5%), *RPS7* (1%), *RPS10* (6.4%), *RPS17* (1%), *RPS24* (2%), and *RPS26* (2.6%).[4-7] To date, approximately half of the DBA patients analyzed have had a mutation in one of these genes. Konno et al screened 49 Japanese patients and found that 30% (12 of 49) carried mutations.[8] In addition, our data showed that 22 of 68 DBA patients (32.4%) harbored a mutation in ribosomal protein (RP) genes (T.T., K.T., R.W., and E.I., unpublished observation, April 16, 2011). These abnormalities of RP genes cause defects in ribosomal RNA processing, formation of either the large or small ribosome subunit, and decreased levels of polysome formation,[4-6,9-12] which is thought to be one of the mechanisms for impairment of erythroid lineage differentiation.

Although sequence analyses of genes responsible for DBA are well established and have been used to identify new mutations, it is estimated that approximately half of the mutations remain to be determined. Because of the difficulty of investigating whole allele deletions, there have been few reports regarding allelic loss in DBA, and they have only been reported for *RPS19* and *RPL35A*.[3,6,13] However, a certain percentage of DBA patients are thought to have a large deletion in RP genes. Therefore, a detailed analysis of allelic loss mutations should be conducted to determine other RP genes that might be responsible for DBA.

In the present study, we investigated large deletions using our novel approach for gene copy number variation analysis based on quantitative-PCR and a single nucleotide polymorphism (SNP) array. We screened Japanese DBA patients and found 7 patients with a large deletion in an allele in *RPL5*, *RPL35A*, *RPS17*, or *RPS19*. Interestingly, all of these patients with a large deletion had a phenotype of growth retardation, including short stature and

Submitted July 24, 2011; accepted November 15, 2011. Prepublished online as *Blood* First Edition paper, January 18, 2012; DOI 10.1182/blood-2011-07-368662.

The online version of this article contains a data supplement.

The publication costs of this article were defrayed in part by page charge payment. Therefore, and solely to indicate this fact, this article is hereby marked "advertisement" in accordance with 18 USC section 1734.

Table 1. Primers used for synchronized quantitative-PCR (s-q-PCR) of RPL proteins

Gene	Primer name	Sequence	Primer name	Sequence	Size, bp
RPL5	L5-02F	CTCCCAAAGTGCTTGAGATTACAG	L5-02R	CACCTTTTCCTAACAAATTCCCAAT	132
	L5-05F	AGCCCTCCAACCTAGGTGACA	L5-05R	GAATTGGGATGGGCAAGAACT	102
	L5-17F	TGAACCCTTGCCCTAAAACATG	L5-17R	TCTTGGTCAGGCCCTGCTTA	105
	L5-19F	ATTGTGCAAACTCGATCACTAGCT	L5-19R	GTGTCTGAGGCTAACACATTTCCAT	103
	L5-21F	GTGCCACTCTCTTGGACAAACTG	L5-21R	CATAGGGCCAAAAGTCAAATAGAAG	102
	L5-28F	TCCACTTTAGGTAGGCGAAACC	L5-28R	TCAGATTTGGCATGTACCTTTCA	102
RPL11	L11-06F	GCACCCACATGGCTTAAAGG	L11-6R	CAACCAACCCATAGGCCAAA	102
	L11-20F	GAGCCCCCTTTCTCAGATGATA	L11-20R	CATGAACTTGGGCTCTGAATCC	109
	L11-22F	TATGTGCAGATAAGAGGGCAGTCT	L11-22R	ATACAGATAAGGAAACTGAGGCAGATT	98
RPL19	L19-02F	TGGCCTCTCATAAAGGAAATCTCT	L19-02R	GGAATGCAGGCAAGTTACTCTGTT	103
	L19-08F	TTTGAAGGCAAGAAATAAGTTCCA	L19-08R	AGCACATCACAGAGTCCAAATAGG	107
	L19-16F	GGTTAGTTGAAGCAGGAGCCTTT	L19-16R	TGCTAGGGAGACAGAAGCACATC	102
	L19-19F	GGACCAGTAGTTGTGACATCAGTTAAG	L19-19R	CCCATTTGTAACCCCCACTTG	106
RPL26	L26-03F	TCCAAAGAGCTGAGACAGAAGTACA	L26-03R	TCCATCAAGACAACGAGAACAAGT	102
	L26-16F	TTTGAGAATGCTTGAGAGAAGGAA	L26-16R	TTCCAGCACATGTAAAATCAAGGA	102
	L26-18F	ATGTTTTAATAAGCCCTCCAGTTGA	L26-18R	GAGAACAGCAAGTTGAAAGGTTCA	102
	L26-20F	GGGCTTTGCTTGATCACTCTAGA	L26-20R	AGGGAGCCCGAAAACATTTAC	104
RPL35A	L35A-01F	TGTGGCTTCTATTTTGCGTCAT	L35A-01R	GGAATTACCTCCTTTATTGCTTACAAG	121
	L35A-07F	TTTCCGTTCTGTCTATTGCTGTGT	L35A-07R	GAACCCTGAGTGGAGGATGTTC	113
	L35A-17F	GCCCACAACCTCCAGAGAATC	L35A-17R	GGATCACTTGAGGCCAGGAAT	104
	L35A-18F	TTAGGTGGGCTTTTCAGTCTCAA	L35A-18R	ATCTCCTGATTCCCCAACTTTGT	102
RPL36	L36-02F	CCGCTCTACAAGTGAAGAAATTCTG	L36-02R	CTCCCTCTGCCTGTGAAATGA	102
	L36-04F	TGCGTCCTGCCAGTGTTG	L36-04R	GGGTAGCTGTGAGAACCAAGGT	105
	L36-17F	CCCCTTGAAAGGACAGCAGTT	L36-17R	TTGGACACCAGGCACAGACTT	114

Table 2. Primers used for s-q-PCR of RPS proteins

Gene	Primer name	Sequence	Primer name	Sequence	Size, bps
RPS7	S7-11F	GCGCTGCCAGATAGGAAATC	S7-11R	TTAGGGAGCTGCCTTACATATGG	102
	S7-12F	ACTGGCAGTTCTGTGATGCTAAGT	S7-12R	ACTCTTGCTCATCTCCAAAACCA	102
	S7-16F	GTGTCTGTGCCAGAAAGCTTGA	S7-16R	GAACCATGCAAAAGTGCCAATAT	112
RPS10	S10-03F	CTACGGTTTTGTGTGGGTCACTT	S10-03R	CATCTGCAAGAAGGAGACGATTG	102
	S10-15F	GTTGGCCTGGAGTCGTGATTT	S10-15R	ATTCCAAGTGCACCATTTCCTT	101
	S10-17F	AATGGTGTTTAGGCCAACGTTAC	S10-17R	TTTGAACAGTGGTTTTTGTGCAT	100
RPS14	S14-03F	GAATTCCAAACCCTTCTGCAAA	S14-03R	TTGCTTCATTTACTCCTCAAGACATT	104
	S14-05F	ACAACCAGCCCTCTACCTCTTTT	S14-05R	GGAAGACGCCGGCATTATT	102
	S14-06F	CGCCTCTACCTCGCCAAAC	S14-06R	GGGATCGGTGCTATTGTTATTCC	102
	S14-09F	GCCATCATGCCGAAACATACT	S14-09R	AACGCGCCACAGGAGAGA	102
	S14-13F	ATCAGGTGGAGCACAGGAAAAC	S14-13R	GCGAGGGAGCTGCTTGATT	111
	S14-15F	AGAAGTTTTAGTGAGGCAGAAATGAGA	S14-15R	TCCCCTGGCTATTAAATGAAACC	102
	S14-19F	GATGAATTGTCCTTTCCTCCATTC	S14-19R	TAGGCGGAAACCAAAAATGCT	102
RPS15	S15-11F	CTCAGCTAATAAAGGCGCACATG	S15-11R	CCTCACACCACGAACCTGAAG	108
	S15-15F	GGTTGGAGAACATGGTGAGAACTA	S15-15R	CACATCCCTGGGCCACTCT	108
RPS17	S17-03F	ACTGCTGTCGTGGCTCGATT	S17-03R	GATGACCTGTTCTTCTGGCCTTA	121
	S17-05F	GAAAACAGATACAAATGGCATGGT	S17-05R	TGCCTCCCACTTTTCCAGAGT	114
	S17-12F	CTATGTGTAGGAGGTCCCAGGATAG	S17-12R	CCACCTGGTACTGAGCACATGT	102
	S17-16F	TAGCGGAAGTTGTGTGCATTG	S17-16R	CAAGAACAGAAGCAGCCAAGAG	102
	S17-18F	TGGCTGAATCTGCCTGCTT	S17-18R	GCCTTGTATGTACCTGGAAATGG	103
	S17-20F	GGGCCCTTCACAAATGTTGA	S17-20R	GCAAAACTCTGTCCCTTTGAGAA	101
RPS19	S19-24F	CCATCCCAAGAATGCACACA	S19-24R	CGCCGTAGCTGGTACTCATG	120
	S19-28F	GACACACCTGTTGAGTCCTCAGAGT	S19-28R	GCTTCTATTAACTGGAGCACACATCT	114
	S19-36F	CTCTTGAGGGTGGTCTGGAAAT	S19-36R	GTCTTTGCGGGTTCTTCCTCTAC	102
	S19-40F	GGAACGGTGTCAGGATTCAAG	S19-40R	AGCGGCTGTACACCAGAAATG	101
	S19-44F	CTGAGGTTGAGTGTCCCATTTCT	S19-44R	GCACCGGGCCTCTGTTATC	104
	S19-57F	CAGGGACACAGTGCTGAGAAACT	S19-57R	TGAGATGTCCCATTTTCACTATTGTT	101
	S19-58F	CATGATGTTAGCTCCGTTGCATA	S19-58R	ATTTTGGGAAGAGTGAAGCTTAGGT	102
	S19-62F	GCAACAGAGCGAGACTCCATTT	S19-62R	AGCACTTTTCGGCACTTACTTCA	102
	S19-65F	ACATTTCCCAGAGCTGACATGA	S19-65R	TCGGGACACCTAGACCTTGCT	102
RPS24	S24-17F	CGACCACGTCTGGCTTAGAGT	S24-17R	CCTTCATGCCCAACCAAGTC	101
	S24-20F	ACAAGTAAGCATCATCACCTCGAA	S24-20R	TTTCCCTCACAGCTATCGTATGG	105
	S24-32F	GGGAAATGCTGTGTCCACATACT	S24-32R	CTGGTTTCATGGCTCCAGAGA	105
RPS26	S26-03F	CGCAGCAGTCAGGGACATTT	S26-03R	AAGTTGGGCGAAGGCTTTAAG	104
	S26-05F	ATGGAGGCCGTCTAGTTTGGT	S26-05R	TGCCTACCCTGAACCTTGCT	102
RPS27A	S27A-09F	GCTGGAGTGCATTCGCTTGT	S27A-09R	CACGCCTGTAATCCCCACTAA	102
	S27A-12F	CAGGCTTGGTGTGCTGTGACT	S27A-12R	ACGTCCATCTTCCAGCTGCTT	103
	S27A-18F	GGGTTTTTCCTGTTTGGTATTTGA	S27A-18R	AAAGGCCAGCTTTGCAAGTG	111
	S27A-22F	TTACCATATTGCCAGTCTTTCCATT	S27A-22R	TTCATATGCATTTGCACAAACTGT	106

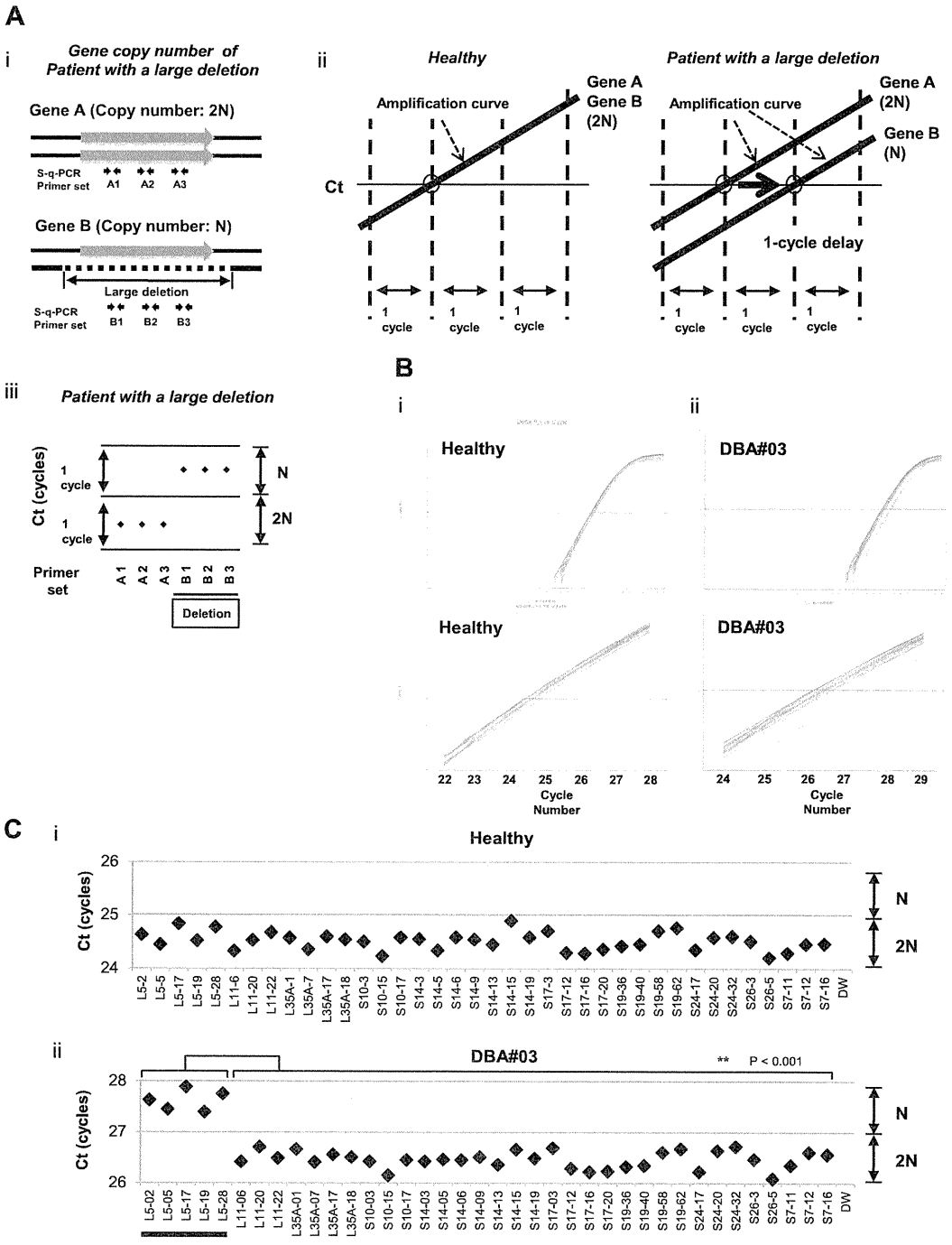

Figure 1. s-q-PCR can determine a large gene deletion in DBA. (A) Concept of the DBA s-q-PCR assay. The difference in gene copy number between a healthy sample and that with a large deletion is 2-fold (i). When all genomic s-q-PCR for genes of interest synchronously amplify DNA fragments, a 2-fold difference in the gene copy number is detected by a 1-cycle difference of the Ct scores of the s-q-PCR amplification curves (ii). Also shown is a dot plot of the Ct scores (iii). (B) Results of the amplification curves of s-q-PCR performed with a healthy person (i) and a DBA patient (patient 3; ii). The top panel shows the results of PCR cycles; the bottom panel is an extended graph of the PCR cycles at logarithmic amplification. (C) Graph showing Ct scores of s-q-PCR. If all specific primer sets for DBA genes show a 1-cycle delay relative to each other, this indicates a large deletion in the gene. Gene primer sets with a large deletion are underlined in the graph. $^{**}P < .001$.

small-for-gestational age (SGA), which suggests that this is a characteristic of DBA patients with a large gene deletion in Japan.

Methods

Patient samples

Genomic DNA was extracted using the GenElute Blood Genomic DNA Kit (Sigma-Aldrich) according to the manufacturer's protocol. Clinical manifestation of patients from a Japanese DBA genomic library are listed elsewhere or are as reported by Konno et al.[8] The study was approved by the institutional review board at the National Institute of Infectious Diseases and Hirosaki University.

DBA gene copy number assay by s-q-PCR

For s-q-PCR, primers were designed using Primer Express Version 3.0 software (Applied Biosystems). Primers are listed in Tables 1 and 2. Genomic DNA in water was denatured at 95°C for 5 minutes and

immediately cooled on ice. The composition of the s-q-PCR mixture was as follows: 5 ng of denatured genomic DNA, 0.4mM forward and reverse primers, 1× SYBR Premix Ex Taq II (Takara), and 1× ROX reference dye II (Takara) in a total volume of 20 μL (all experiments were performed in duplicate). Thermal cycling was performed using the Applied Biosystems 7500 fast real-time PCR system. Briefly, the PCR mixture was denatured at 95°C for 30 seconds, followed by 35 cycles of 95°C for 5 seconds, 60°C for 34 seconds, and then dissociation curve measurement. Threshold cycle (Ct) scores were determined as the average of duplicate samples. The technical errors of Ct scores in the triplicate analysis were within 0.2 cycles (supplemental Figure 1, available on the *Blood* Web site; see the Supplemental Materials link at the top of the online article). The sensitivity and specificity of this method was evaluated with 15 healthy samples. Any false positive was not observed in all primer sets in all healthy samples (supplemental Figure 2). We performed direct sequencing of the s-q-PCR products. The results of the sequence analysis were searched for using BLAST to confirm uniqueness. Sequence data were obtained from GenBank (http://www.ncbi.nlm.nih.gov/gene/) and Ensemble Genome Browser (http://uswest.ensembl.org).

Genomic PCR

Genomic PCR was performed using KOD FX (Toyobo) according to the manufacturer's step-down PCR protocol. Briefly, the PCR mixture contained 20 ng of genomic DNA, 0.4mM forward and reverse primers, 1mM dNTP, 1× KOD FX buffer, and 0.5 U KOD FX in a total volume of 25 μL in duplicate. Primers are given in supplemental Figure 3 and Table 2. PCR mixtures were denatured at 94°C for 2 minutes, followed by 4 cycles of 98°C for 10 seconds, 74°C for 12 minutes, followed by 4 cycles of 98°C for 10 seconds, 72°C for 12 minutes followed by 4 cycles of 98°C for 10 seconds, 70°C for 12 minutes, followed by 23 cycles of 98°C for 10 seconds and 68°C for 12 minutes. PCR products were loaded on 0.8% agarose gels and detected by LAS-3000 (Fujifilm).

DNA sequencing analysis

The genomic PCR product was purified by the GenElute PCR clean-up kit (Sigma-Aldrich) according to the manufacturer's instructions. Direct sequencing was performed using the BigDye Version 3 sequencing kit. Sequences were read and analyzed using a 3120x genetic analyzer (Applied Biosystems).

SNP array-based copy number analysis

SNP array experiments were performed according to the standard protocol of GeneChip Human Mapping 250K Nsp arrays (Affymetrix). Microarray data were analyzed for determination of the allelic-specific copy number using the CNAG program, as described previously.[14] All microarray data are available at the EGA database (www.ebi.ac.uk/ega) under accession number EGAS00000000105.

Results

Construction of a convenient method for RP gene copy number analysis based on s-q-PCR

We focused on the heterozygous large deletions in DBA-responsible gene. The difference in copy number of genes between a mutated DBA allele and the intact allele was 2-fold (N and 2N; Figure 1Ai). If each PCR can synchronously amplify DNA fragments when the template genomic DNA used is of normal karyotype, it is possible to conveniently detect a gene deletion with a 1-cycle delay in s-q-PCR analysis (Figure 1Aii-iii).

Table 3. Summary of mutations and the mutation rate observed in Japanese DBA patients

Gene	Sequencing analysis
RPS19	10
RPL5	6
RPL11	3
RPS17	1
RPS10	1
RPS26	1
RPL35A	0
RPS24	0
RPS14	0
Mutations, n (%)	22 (32.4%)
Total analyzed, N	68

To apply this strategy for allelic analysis of DBA, we prepared primers for 16 target genes, *RPL5*, *RPL11*, *RPL35A*, *RPS10*, *RPS19*, *RPS26*, *RPS7*, *RPS17*, *RPS24*, *RPL9*, *RPL19*, *RPL26*, *RPL36*, *RPS14*, *RPS15*, and *RPS27A*, under conditions in which the Ct of s-q-PCR would occur within 1 cycle of that of the other primer sets (Tables 1 and 2). At the same time, we defined the criteria of a large deletion in our assay as follows. If multiple primer sets for one gene showed a 1-cycle delay from the other gene-specific primer set at the Ct score, we assumed that this represented a large deletion. As shown in Figure 1Bii and 1Cii, the specific primer sets for *RPL5* (L5-02, L5-05, L5-17, L5-19, and L5-28) detected a 1-cycle delay with respect to the mutated allele of patient 3. This assessment could be verified by simply confirming the difference of the cycles with the s-q-PCR amplification curves.

Study of large gene deletions in a Japanese DBA genomic DNA library

Sixty-eight Japanese DBA patients were registered and blood genomic DNA was collected at Hirosaki University. All samples were first screened for mutations in *RPL5*, *L11*, *L35A*, *S10*, *S14*, *S17*, *S19*, and *S26* by sequencing. Among these patients, 32.4% (22 of 68) had specific DBA mutations (Table 3 and data not shown). We then screened for large gene deletions in 27 patients from the remaining 46 patients who did not possess mutations as determined by sequencing (Table 4).

When we performed the s-q-PCR DBA gene copy number assay, 7 of 27 samples displayed a 1-cycle delay of Ct scores: 1 patient had *RPL5* (patient 14), 1 had *RPL35A* (patient 71), 3 had *RPS17* (patients 3, 60, 62), and 2 had *RPS19* (patients 24 and 72; Figure 2 and Table 4). Among these patients, the large deletions in the *RPL5* and *RPS17* genes are the first reported cases of allelic deletions in DBA. From these results, we estimate that a sizable number of Japanese DBA patients have a large deletion.

Based on our findings, the rate of large deletions was approximately 25.9% (7 of 27) in a category of unspecified gene mutations. Such mutations have typically gone undetected by conventional sequence analysis. We could not find any additional gene deletions in the analyzed samples.

Confirmation of the gene copy number for DBA genes by genome-wide SNP array

We performed genome-wide copy number analysis of the 27 DBA patients with a SNP array to confirm our s-q-PCR results. SNP array showed that patient 3 had a large deletion in

Table 4. Characteristics of DBA patients tested

Patient no.	Age at diagnosis	Sex	Hb, g/dL	Large deletion by s-q-PCR	Large deletion by SNP array	Inheritance	Malformations	Response to first steroid therapy
Patients with a large deletion in RP genes								
3*†	1 y	M		RPL5	RPL5	Sporadic	Short stature, thumb anomalies	Response
14*	5 y	M	5.5	RPS17	RPS17	Sporadic	White spots, short stature	Response
24*†	1 mo	F	5.5	RPS19	ND	Sporadic	Short stature, SGA	Response
60*†	2 mo	F	2.4	RPS17	RPS17	Sporadic	SGA	NT
62*†	1 mo	F	6.2	RPS17	RPS17	Sporadic	Small ASD, short stature, SGA	Response
71	0 y	M	5.3	RPL35A	RPL35A	Sporadic	Thumb anomalies, synostosis of radius and ulna, Cohelia Lange-like face, cleft palate, underdescended testis, short stature, cerebellar hypoplasia, fetal hydrops	NT
72†	0 y	M	2	RPS19	RPS19	Sporadic	Thumb anomalies, flat thenar, testicular hypoplasia, fetal hydrops, short stature, learning disability	No
Patients without a large deletion in RP genes								
5*	1 y	F	3.1	ND	ND	Sporadic	ND	Response
15*	1 mo	F	1.6	ND	ND	Sporadic	ND	Response
21*	1 y	F	2.6	ND	ND	Sporadic	ND	Response
26*	1 y 1 mo	F	8	ND	ND	Sporadic	Congenital hip dislocation, spastic quadriplegia, hypertelorism, nystagmus, short stature, learning disability	Response
33*	2 mo	F	1.3	ND	ND	Sporadic	ND	Response
36*	0 y	M	8.2	ND	ND	Familial	ND	Response
37*	4 y	M	6.1	ND	ND	Sporadic	Hypospadias, underdescended testis, SGA	NT
45*	5 d	M	5.1	ND	ND	Sporadic	Short stature, microcephaly, mental retardation, hypogammaglobulinemia	Poor
50*	2 m	F	3.4	ND	ND	Familial	ND	Response
61*	9 m	M	4	ND	ND	Sporadic	ND	Response
63*	0 y	M	6.8	ND	ND	Sporadic	Micrognathia, hypertelorism, short stature	Response
68	1 y 4 mo	M	5.9	ND	ND	Sporadic	ND	NT (CR)
69	1 y	M	9.3	ND	ND	Sporadic	ND	Response
76	0 y	M	4	ND	ND	Sporadic	ND	Response
77	0 y	M	7.8	ND	ND	Familial	Short stature	No
83	9 mo	F	3	ND	ND	Sporadic	ND	NT
90	10 mo	M	9	ND	ND	Sporadic	ND	No
91	0 y	F	3.8	ND	ND	Sporadic	ND	Response
92	2 mo	M	3.7	ND	ND	Sporadic	ASD, PFO, melanosis, underdescended testis, SGA, short stature	Response
93	11 mo	M	2.2	ND	ND	Sporadic	White spots, senile face, corneal opacity, underdescended testis, syndactyly, ectrodactyly, flexion contracture, extension contracture	Response

ND indicates not detected; NT, not tested; CR, complete remission; ASD, atrial septal defect; and PFO, persistent foramen ovale.

*Status data of Japanese probands 3 to 63 is from a report by Konno et al.[8]

†Large deletions of the parents of 5 DBA patients (3, 24, 60, 62, and 72) were analyzed by s-q-PCR, but there were no deletions in DBA genes in any of the 5 pairs of parents.

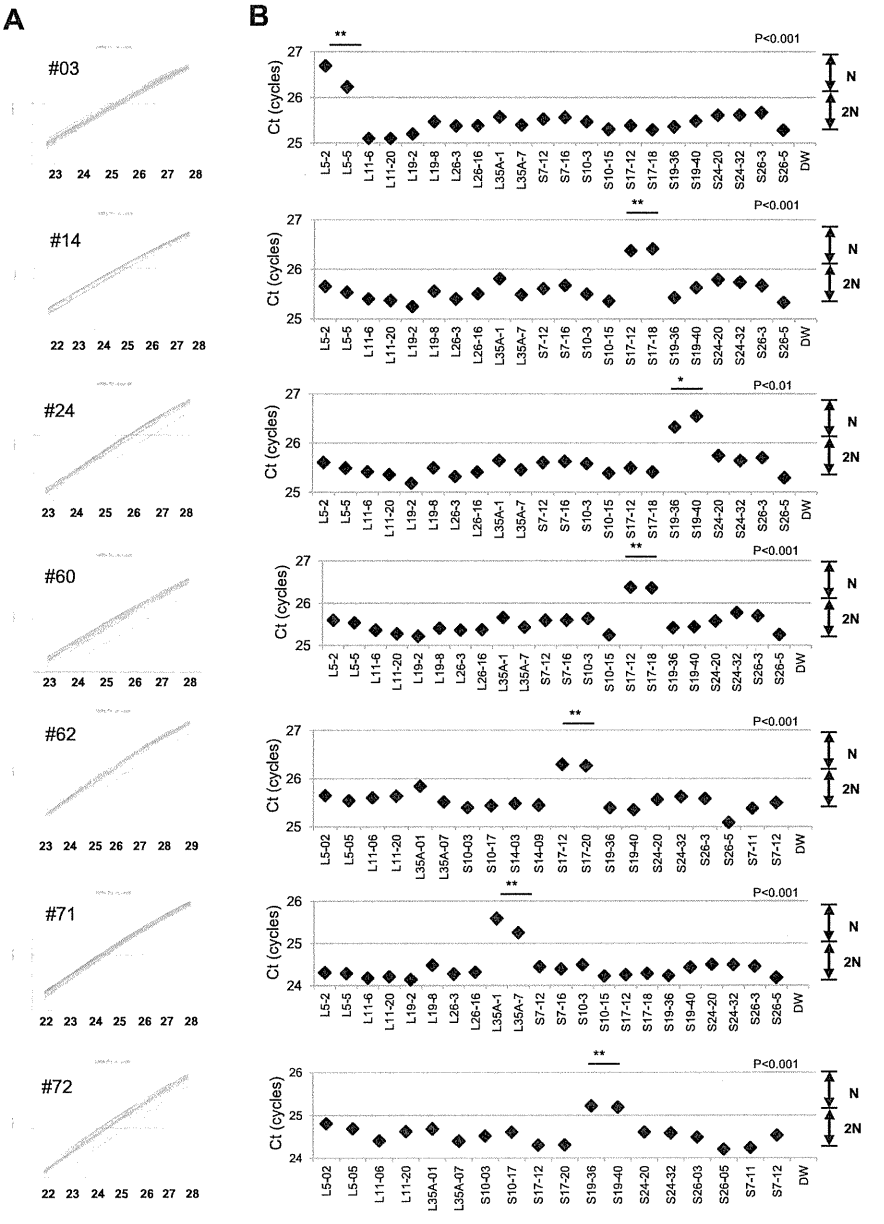

Figure 2. Detection of 7 mutations with a large deletion in DBA patients. Genomic DNA of 27 Japanese DBA patients with unknown mutations were subjected to the DBA gene copy number assay. (A) Amplification curve of s-q-PCR of a mutation with a large deletion. The deleted gene can be easily distinguished. (B) Ct score (cycles) of representative s-q-PCR with DBA genomic s-q-PCR primers. Results of the 2 gene-specific primer pairs indicated in the graph are representative of at least 2 sets for each gene-specific primer (carried out in the same run). $^{**}P < .001$; $^{*}P < .01$

chromosome 1 (ch1) spanning 858 kb (Figure 3A); patient 71 had a large deletion in ch3 spanning 786 kb (Figure 3B); patients 14, 60, and 62 had a large deletion in ch15 spanning 270 kb, 260 kb, and 330 kb, respectively (Figure 3C); and patient 72 had a large deletion in ch19 spanning 824 kb (Figure 3D). However, there were no deletions detected in ch19 in patient 24 (Figure 3D). Genes estimated to reside within a large deletion are listed in supplemental Table 1. Consistent with these s-q-PCR results, 6 of 7 large deletions were detected and confirmed as deleted regions, and these large deletions contained *RPL5*, *RPL35A*, *RPS17*, and *RPS19* (Table 4 and supplemental Table 1). Other large deletions in RP genes were not detected by this analysis. From these results, we conclude that the synchronized multiple PCR amplification method has a detection sensitivity comparable to that of SNP arrays.

Detailed examination of a patient with intragenic deletion in the RPS19 allele (patient 24)

Interestingly, for patient 24, in whom we could not detect a large deletion by SNP array at s-q-PCR gene copy number analysis, 2 primer sets for *RPS19* showed a 1-cycle delay (RPS19-36 and RPS19-40), but 2 other primer pairs (RPS19-58 and RPS19-62) did not show this delay (Figure 4A). We attempted to determine the deleted region in detail by testing more primer sets on *RPS19*. We tested a total of 9 primer sets for *RPS19* (Figure 4B) and examined the gene copy numbers. Surprisingly, 4 primer sets (S19-24, S19-36, S19-40, and S19-44) for intron 3 of *RPS19* indicated a 1-cycle delay, but the other primers for *RPS19* located on the 5′untranslated region (5′UTR), intron 3, or 3′UTR did not show this delay (S19-57, S19-58, S19-28, S19-62, and S19-65; Figure 4B-C). These results suggest that the intragenic deletion occurred in the *RPS19* allele. To confirm this deleted region precisely, we performed genomic PCR on *RPS19*, amplifying a region from the 5′UTR to intron 3 (Figure

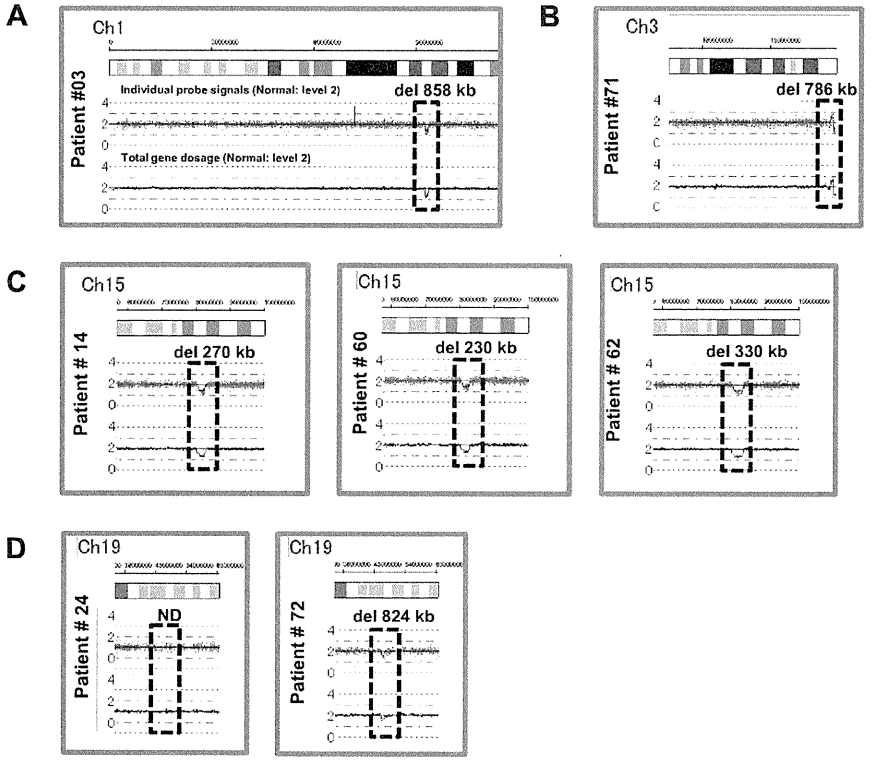

Figure 3. Results of SNP genomic microarray (SNP-chip) analysis. Genomic DNA of 27 Japanese DBA patients with unknown mutations was examined using a SNP array. Six patients had large deletions in their chromosome (ch), which included one DBA-responsible gene. Patient 3 has a large deletion in ch1 (A), patient 71 has a deletion in ch3 (B), patients 14, 60, and 62 have deletions in ch15 (C), and patient 72 has a deletion in ch19 (D).

4B). In patient 24, we observed an abnormally sized PCR product at a low molecular weight by agarose gel electrophoresis (Figure 4D). We did not detect a wild-type PCR product from the genomic PCR. This finding is probably because PCR tends to amplify smaller molecules more easily. However, we did detect a PCR fragment at the correct size using primers located in the supposedly deleted region. These bands were thought to be from the products of a wild-type allele. Sequencing of the mutant band revealed that intragenic recombination occurred at a homologous region of 27 nucleotides, from −1400 to −1374 in the 5′ region, to +5758 and +5784 in intron 3, which resulted in the loss of 7157 base pairs in the *RPS19* gene (Figure 4E). The deleted region contains exons 1, 2, and 3, and therefore the correct *RPS19* mRNA could not be transcribed.

Genotype-phenotype analysis and DBA mutations in Japan

Patients with a large deletion in DBA genes had common phenotypes (Table 4). Malformation with growth retardation (GR), including short stature or SGA, were observed in all 7 patients. In patients who had a mutation found by sequencing, half had GR (11 of 22; status data of DBA patients with mutations found by sequencing are not shown). GR may be a distinct phenotypic feature of large deletion mutations in Japanese DBA patients. Familial mutations were analyzed for parents for 5 DBA patients with a large deletion (patients 3, 24, 60, 62, and 72) by s-q-PCR. There are no large deletions in all 5 pairs of parents in DBA-responsible genes. Four of the 7 patients responded to steroid therapy. We have not observed significant phenotypic differences between patients with extensive deletions and other patients with regard to blood counts, responsiveness to treatment, or other malformations.

Discussion

Many studies have reported RP genes to be responsible for DBA. However, mutations have not been determined for approximately half of DBA patients analyzed. There are 2 possible reasons for this finding. One possibility is that patients have other genes responsible for DBA, and the other is that patients have a complicated set of mutations in RP genes that are difficult to detect. In the present study, we focused on the latter possibility because we have found fewer Japanese DBA patients with RP gene mutations (32.4%) compared with another cohort study of 117 DBA patients and 9 RP genes (approximately 52.9%).[4] With our newly developed method, we identified 7 new mutations with a large deletion in *RPL5*, *RPL35A*, *RPS17*, and *RPS19*.

The frequency of a large deletion was approximately 25.9% (7 of 27) in our group of patients who were not found to have mutations by genomic sequencing. Therefore, total RP gene mutations were confirmed in 42.6% of these Japanese patients (Table 5). Interestingly, mutations in *RPS17* have been observed at a high rate (5.9%) in Japan relative to that in other countries (1%).[5,15,16] Although the percentage of DBA mutations differs among different ethnic groups,[8,17-19] a certain portion of large deletions in DBA-responsible genes are likely to be determined in other countries by new strategies.

In the present study, we analyzed patient data to determine genotype-phenotype relations. To date, large deletions have been reported with RPS19 and RPL35A in DBA patients.[3,6,13] *RPS19* large deletions/translocations have been reported in 12 patients, and *RPL35A* large deletions have been reported in 2 patients.[19] GR in patients with a large deletion has been observed previously with *RPS19* translocations,[3,19-21] but it was not found in 2 patients with *RPL35A* deletion.[6] Interestingly, all of our patients with a large deletion had a phenotype

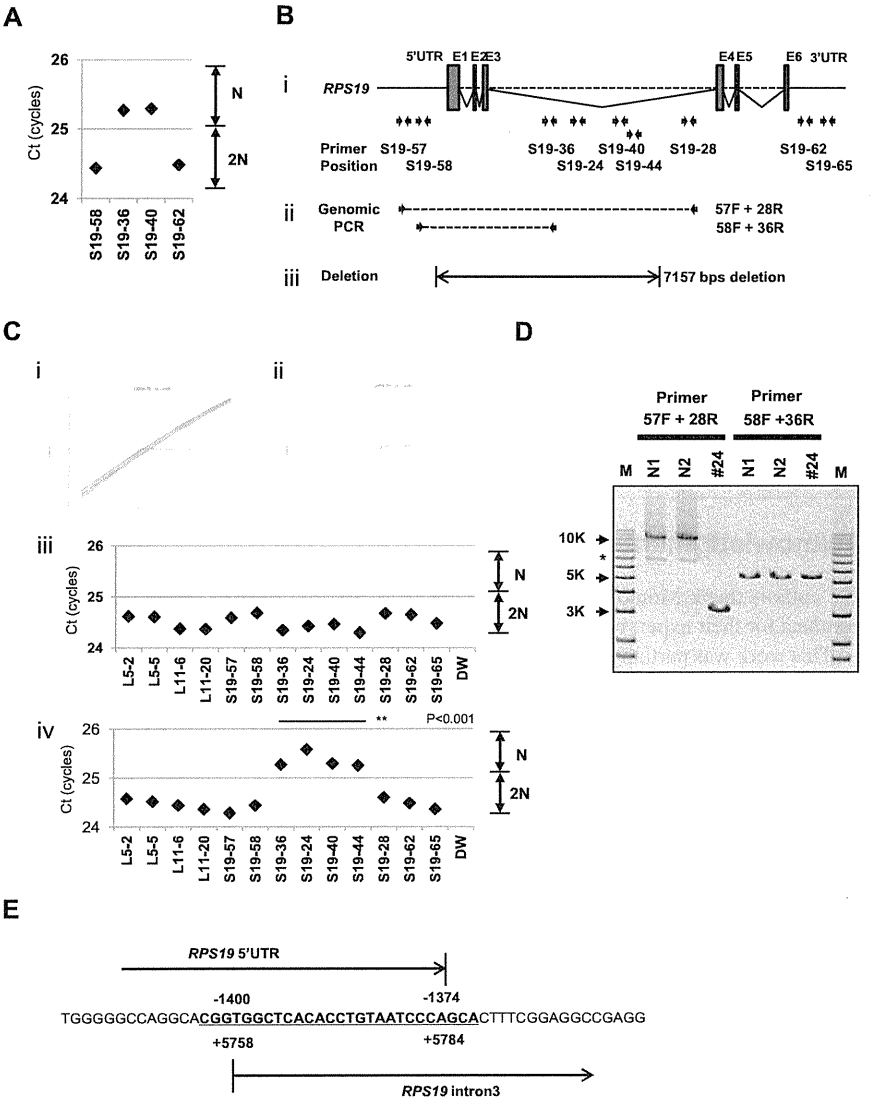

Figure 4. Result of s-q-PCR gene copy number assay for patient 24. (A) Results of s-q-PCR gene copy number assay for *RPS19* with 4 primer sets. (Bi) The *RPS19* gene copy number was analyzed with 9 specific primer sets for *RPS19* that span from the 5′UTR to the 3′UTR. (ii) Primer positions of genomic PCR for *RPS19*. (iii) Region determined to be an intragenic deletion in *RPS19*. (C) Results of gene copy number assay for *RPS19* show a healthy person (i,iii) and a DBA patient (ii,iv), and Ct results are shown (iii-iv). Patient 24 showed a "1-cycle delay" with primers located in the intron 3 region, but other primer sets were normal. (D) Results of genomic PCR amplification visualized by agarose gel electrophoresis to determine the region of deletion. N1 and N2 are healthy samples. *Nonspecific band. (E) Results from the genomic sequence of the 3-kb DNA band from genomic PCR on patient 24 showing an intragenic recombination from −1400 to 5784 (7157 nt) in *RPS19*. $^{**}P < .001$.

of GR, including short stature and SGA, which suggests that this is a characteristic of DBA with a large gene deletion in Japan. Our study results suggest the possibility that GR is associated with extensive deletion in Japanese patients. Although further case studies will be needed to confirm this possibility, screening of DBA samples using our newly developed method will help to advance our understanding of the broader implications of the mutations and the correlation with the DBA genotype-phenotype.

Table 5. Total mutations in Japanese DBA patients, including large gene deletions

Gene	Mutation rate
RPS19	12(17.6%)
RPL5	7(10.3%)
RPL11	3 (4.4%)
RPS17	4 (5.9%)
RPS10	1 (1.5%)
RPS26	1 (1.5%)
RPL35A	1 (1.5%)
RPS24	0
RPS14	0
Mutations, n (%)	29(42.6%)
Total analyzed, N	68

Copy number variation analysis of DBA has been performed by linkage analysis, and the *RPS19* gene was first identified as a DBA-susceptibility gene. Comparative genomic hybridization array technology has also been used to detect DBA mutations in *RPL35A*, and multiplex ligation-dependent probe amplification has been used for *RPS19* gene deletion analysis.[3,6,13,22] However, these analyzing systems have problems in mutation screening. Linkage analysis is not a convenient tool to screen for multiple genetic mutations, such as those in DBA, because it requires a high level of proficiency. Although comparative genomic hybridization technology is a powerful tool with which to analyze copy number comprehensively, this method requires highly specialized equipment and analyzing software, which limits accessibility for researchers. Whereas quantitative PCR–based methods for copy number variation analysis are commercially available (TaqMan), they require a standard curve for each primer set, which limits the number of genes that can be loaded on a PCR plate. To address this issue, a new method of analysis is needed. By stringent selection of PCR primers, the s-q-PCR method enables analysis of many DBA genes in 1 PCR plate and the ability to immediately distinguish a large deletion using the s-q-PCR amplification curve. In our study, 6 of 7 large deletions in the RP gene detected by s-q-PCR were confirmed by SNP arrays (Figure 3). Interestingly, we detected

1 large intragenic deletion in *RPS19*, which was not detected by the SNP array. This agreement between detection results suggests that the s-q-PCR copy number assay could be useful for detecting large RP gene deletions.

In the present study, 7 DBA patients carried a large deletion in the RP genes. This type of mutation could be underrepresented by sequencing analysis, although in the future, genome sequencing might provide a universal platform for mutation and deletion detection. We propose that gene copy number analysis for known DBA genes, in addition to direct sequencing, should be performed to search for a novel responsible gene for DBA. Although at present, it may be difficult to observe copy numbers on all 80 ribosomal protein genes in one s-q-PCR assay, our method allows execution of gene copy number assays for several target genes in 1 plate. Because our method is quick, easy, and low cost, it could become a conventional tool for detecting DBA mutations.

Acknowledgments

The authors thank Momoka Tsuruhara, Kumiko Araki, and Keiko Furuhata for their expert assistance.

This work was partially supported by grants-in-aid for scientific research from the Ministry of Education, Culture, Sports, Science and Technology of Japan, and by Health and Labor Sciences research grants (Research on Intractable Diseases) from the Ministry of Health, Labor and Welfare of Japan.

Authorship

Contribution: M.K. designed and performed the research, analyzed the data, and wrote the manuscript; A.S-O. and S. Ogawa performed the SNP array analysis; T.M., M.T., and M.O designed the study; T.T, K. Terui, and R.W. analyzed the mutations and status data; H.K., S. Ohga, A.O., S.K., T.K., K.G., K.K., T.M., and N.M. analyzed the status data; A.M., H.M., K. Takizawa, T.M., and K.Y., performed the research and analyzed the data; E.I. and I.H. designed the study and analyzed the data; and all authors wrote the manuscript.

Conflict-of-interest disclosure: The authors declare no competing financial interests.

Correspondence: Isao Hamaguchi, MD, PhD, Department of Safety Research on Blood and Biological Products, National Institute of Infectious Diseases, 4-7-1, Gakuen, Musashimurayama, Tokyo 208-0011, Japan; e-mail: 130hama@nih.go.jp; or Etsuro Ito, MD, PhD, Department of Pediatrics, Hirosaki University Graduate School of Medicine, 5 Zaifucho, Hirosaki, Aomori 036-8562, Japan; e-mail: eturou@cc.hirosaki-u.ac.jp.

References

1. Hamaguchi I, Flygare J, Nishiura H, et al. Proliferation deficiency of multipotent hematopoietic progenitors in ribosomal protein S19 (RPS19)-deficient diamond-Blackfan anemia improves following RPS19 gene transfer. *Mol Ther.* 2003;7(5 pt 1):613-622.
2. Vlachos A, Ball S, Dahl N, et al. Diagnosing and treating Diamond Blackfan anaemia: results of an international clinical consensus conference. *Br J Haematol.* 2008;142(6):859-876.
3. Draptchinskaia N, Gustavsson P, Andersson B, et al. The gene encoding ribosomal protein S19 is mutated in Diamond-Blackfan anaemia. *Nat Genet.* 1999;21(2):169-175.
4. Doherty L, Sheen MR, Vlachos A, et al. Ribosomal protein genes RPS10 and RPS26 are commonly mutated in Diamond-Blackfan anemia. *Am J Hum Genet.* 2010;86(2):222-228.
5. Gazda HT, Sheen MR, Vlachos A, et al. Ribosomal protein L5 and L11 mutations are associated with cleft palate and abnormal thumbs in Diamond-Blackfan anemia patients. *Am J Hum Genet.* 2008;83(6):769-780.
6. Farrar JE, Nater M, Caywood E, et al. Abnormalities of the large ribosomal subunit protein, Rpl35a, in Diamond-Blackfan anemia. *Blood.* 2008;112(5):1582-1592.
7. Gazda HT, Grabowska A, Merida-Long LB, et al. Ribosomal protein S24 gene is mutated in Diamond-Blackfan anemia. *Am J Hum Genet.* 2006;79(6):1110-1118.
8. Konno Y, Toki T, Tandai S, et al. Mutations in the ribosomal protein genes in Japanese patients with Diamond-Blackfan anemia. *Haematologica.* 2010;95(8):1293-1299.
9. Robledo S, Idol RA, Crimmins DL, Ladenson JH, Mason PJ, Bessler M. The role of human ribosomal proteins in the maturation of rRNA and ribosome production. *RNA.* 2008;14(9):1918-1929.
10. Léger-Silvestre I, Caffrey JM, Dawaliby R, et al. Specific Role for Yeast Homologs of the Diamond Blackfan Anemia-associated Rps19 Protein in Ribosome Synthesis. *J Biol Chem.* 2005;280(46):38177-38185.
11. Choesmel V, Fribourg S, Aguissa-Toure AH, et al. Mutation of ribosomal protein RPS24 in Diamond-Blackfan anemia results in a ribosome biogenesis disorder. *Hum Mol Genet.* 2008;17(9):1253-1263.
12. Flygare J, Aspesi A, Bailey JC, et al. Human RPS19, the gene mutated in Diamond-Blackfan anemia, encodes a ribosomal protein required for the maturation of 40S ribosomal subunits. *Blood.* 2007;109(3):980-986.
13. Quarello P, Garelli E, Brusco A, et al. Multiplex ligation-dependent probe amplification enhances molecular diagnosis of Diamond-Blackfan anemia due to RPS19 deficiency. *Haematologica.* 2008;93(11):1748-1750.
14. Yamamoto G, Nannya Y, Kato M, et al. Highly sensitive method for genomewide detection of allelic composition in nonpaired, primary tumor specimens by use of affymetrix single-nucleotide-polymorphism genotyping microarrays. *Am J Hum Genet.* 2007;81(1):114-126.
15. Song MJ, Yoo EH, Lee KO, et al. A novel initiation codon mutation in the ribosomal protein S17 gene (RPS17) in a patient with Diamond-Blackfan anemia. *Pediatr Blood Cancer.* 2010;54(4):629-631.
16. Cmejla R, Cmejlova J, Handrkova H, Petrak J, Pospisilova D. Ribosomal protein S17 gene (RPS17) is mutated in Diamond-Blackfan anemia. *Hum Mutat.* 2007;28(12):1178-1182.
17. Cmejla R, Cmejlova J, Handrkova H, et al. Identification of mutations in the ribosomal protein L5 (RPL5) and ribosomal protein L11 (RPL11) genes in Czech patients with Diamond-Blackfan anemia. *Hum Mutat.* 2009;30(3):321-327.
18. Quarello P, Garelli E, Carando A, et al. Diamond-Blackfan anemia: genotype-phenotype correlations in Italian patients with RPL5 and RPL11 mutations. *Haematologica.* 2010;95(2):206-213.
19. Boria I, Garelli E, Gazda HT, et al. The ribosomal basis of Diamond-Blackfan Anemia: mutation and database update. *Hum Mutat.* 2010;31(12):1269-1279.
20. Campagnoli MF, Garelli E, Quarello P, et al. Molecular basis of Diamond-Blackfan anemia: new findings from the Italian registry and a review of the literature. *Haematologica.* 2004;89(4):480-489.
21. Willig TN, Draptchinskaia N, Dianzani I, et al. Mutations in ribosomal protein S19 gene and diamond blackfan anemia: wide variations in phenotypic expression. *Blood.* 1999;94(12):4294-4306.
22. Gustavsson P, Garelli E, Draptchinskaia N, et al. Identification of microdeletions spanning the Diamond-Blackfan anemia locus on 19q13 and evidence for genetic heterogeneity. *Am J Hum Genet.* 1998;63(5):1388-1395.

Brief report

Identification of *TRIB1* R107L gain-of-function mutation in human acute megakaryocytic leukemia

Takashi Yokoyama,[1] Tsutomu Toki,[2] Yoshihiro Aoki,[2] Rika Kanezaki,[2] Myoung-ja Park,[3] Yohei Kanno,[1] Tomoko Takahara,[1] Yukari Yamazaki,[1] Etsuro Ito,[2] Yasuhide Hayashi,[3] and Takuro Nakamura[1]

[1]Division of Carcinogenesis, Cancer Institute, Japanese Foundation for Cancer Research, Tokyo, Japan; [2]Department of Pediatrics, Hirosaki University Graduate School of Medicine, Hirosaki, Japan; and [3]Department of Hematology/Oncology, Gunma Children's Medical Center, Gunma, Japan

***Trib1* has been identified as a myeloid oncogene in a murine leukemia model. Here we identified a *TRIB1* somatic mutation in a human case of Down syndrome–related acute megakaryocytic leukemia. The mutation was observed at well-conserved arginine 107 residue in the pseudokinase domain. This R107L mutation remained in leukocytes of the remission stage in which *GATA1* mutation disappeared, suggesting the *TRIB1* mutation is an earlier genetic event in leukemogenesis. The bone marrow transfer experiment showed that acute myeloid leukemia development was accelerated by transducing murine bone marrow cells with the R107L mutant in which enhancement of ERK phosphorylation and C/EBPα degradation by Trib1 expression was even greater than in those expressing wild-type. These results suggest that TRIB1 may be a novel important oncogene for Down syndrome–related acute megakaryocytic leukemia. (*Blood*. 2012; 119(11):2608-2611)**

Introduction

The Down syndrome (DS) patients are predisposed to developing myeloid leukemia, and those patients frequently exhibit *GATA1* mutations.[1] However, it is proposed that the *GATA1* mutation is important for transient leukemia in DS but not sufficient for full-blown leukemia, suggesting that additional genetic alterations are needed.[1] Therefore, it is important to search the subsequent genetic changes for DS-related leukemia (ML-DS) to predict malignant transformation and prognosis of the patients.

Trib1 has been identified as a myeloid oncogene that cooperates with *Hoxa9* and *Meis1* in murine acute myeloid leukemia (AML).[2] As a member of the tribbles family of proteins, TRIB1 interacts with MEK1 and enhances ERK phosphorylation.[2,3] Moreover, TRIB1 promotes degradation of C/EBP family transcription factors, including C/EBPα, an important tumor suppressor for AML, and we observed that degradation of C/EBPα by Trib1 is mediated by its interaction with MEK1.[4] Thus, TRIB1 plays an important role in the development of AML by modulating both the RAS/MAPK pathway and C/EBPα function together with Trib2 that has also been identified as a myeloid-transforming gene.[5] Potential involvement of *TRIB1* in human leukemia has been reported in cases of AML with 8q34 amplification in which both *c-MYC* and *TRIB1* are included in the amplicon.[6] The enhancing effect of TRIB1 on the MAPK signaling suggests that TRIB1 alterations may be related to AML cases, which do not show any mutations in the pathway members, such as FLT3, c-Kit, or Ras. In this report, we identified a novel somatic mutation of *TRIB1* in a case of human acute megakaryocytic leukemia developed in DS (DS-AMKL). Retrovirus-mediated gene transfer followed by bone marrow transfer indicated that the mutation enhanced leukemogenic activity and MAPK phosphorylation by TRIB1.

Methods

Patients

TRIB1 mutations have been investigated in 12 cases of transient leukemia (TL), 5 of DS-AMKL, and 4 cell lines of DS-AML. Peripheral blood leukocytes of TL and bone marrow cells of DS-AMKL were used as sources for the molecular analysis. This study was approved by the Ethics Committee of Hirosaki University Graduate School of Medicine, and all clinical samples were obtained with informed consent from the parents of all patients, in accordance with the Declaration of Helsinki.

Patient 84 showed trisomy 21 and extensive leukocytosis at birth. Hematologic findings revealed the white blood cell count to be 148×10^9/L, including 87% myeloblasts, a hemoglobin level of 19.4 g/dL, and a platelet count of 259×10^9/L. Patent ductus arteriosus and atrial septal defect have been pointed out. Based on the hematologic data and the chromosomal abnormality, the patient was diagnosed as DS-related TL. The hematologic abnormality was then improved, but 8 months later 3% of 6.9×10^9/L white blood cells became myeloblasts (Figure 1A). A karyotype analysis of bone marrow cells revealed 48, XY,+8,+21 in 3 of 20 cells. In addition, *GATA1* mutation was detected at nt 113 from A to G, resulting in loss of the first methionine.[7] He was diagnosed as AMKL at this time, and his disease was in remission by subsequent chemotherapy.

PCR and sequencing

The entire coding region of human *TRIB1* cDNA of patients' samples was amplified using Taq polymerase (Promega) and specific primer pairs (the sequences of the primers are available on request). The genomic DNA samples of patient 84 were also analyzed. The sequence analysis of *GATA1* was performed as described previously.[7] After checking the PCR products by agarose gel electrophoresis, the products were purified and directly sequenced.

Submitted December 12, 2010; accepted January 6, 2012. Prepublished online as *Blood* First Edition paper, January 31, 2012; DOI 10.1182/blood-2010-12-324806.

The online version of this article contains a data supplement.

The publication costs of this article were defrayed in part by page charge payment. Therefore, and solely to indicate this fact, this article is hereby marked "advertisement" in accordance with 18 USC section 1734.

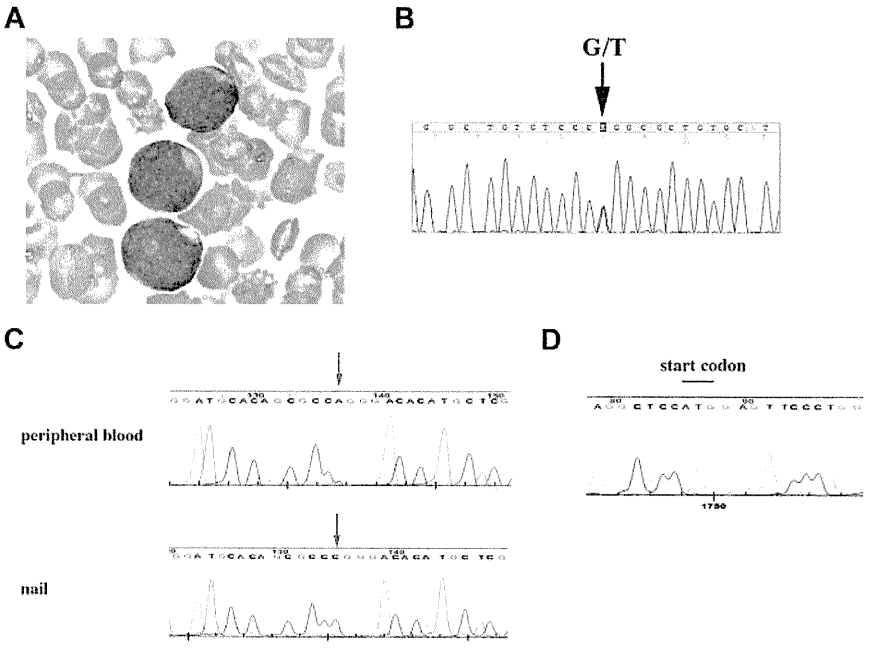

Figure 1. *TRIB1* R107L mutation identified in DS-related leukemias. (A) Giemsa staining of the case 84 peripheral blood smear diagnosed as AMKL. The image was acquired using a BX40 microscope equipped with a 100×/1.30 NA oil objective (Olympus) and a C-4040 digital camera (Olympus). (B) Fluorescent dye sequencing chromatographs of *TRIB1* genotyping by direct sequencing of the case 84 using a cDNA sample as a template. The vertical arrow indicates mixed G and T signals at codon 107. (C) Fluorescent dye sequencing chromatographs of *TRIB1* of peripheral blood leukocytes (top) or nail (bottom) in the same case at the complete remission stage. The red arrows indicate that the mutation remains in leukocytes but not in nail. The reverse strand sequences are shown. (D) *GATA1* sequence. The start codon that was mutated in AMKL[7] is normal in the peripheral blood leukocytes at the remission stage.

Retroviral infection of murine bone marrow cells and bone marrow transfer

Bone marrow cells were prepared from 8-week-old female C57Bl/6J mice 5 days after injection of 150 mg/kg body weight of 5-fluorouracil (Kyowa Hakko Kogyo). Retroviral infection of bone marrow cells and bone marrow transfer experiments were performed as described.[2] Transduction efficiencies evaluated by flow cytometric techniques were comparable between wild-type (WT; 5.3%) and R107L (3.4%). Animals were housed, observed daily, and handled in accordance with the guidelines of the animal care committee at Japanese Foundation for Cancer Research. All the diseased mice were subjected to autopsy and analyzed morphologically, and the blood was examined by flow cytometric techniques. The mice were diagnosed as positive for AML according to the classification of the Bethesda proposal.[8] The survival rate of each group was evaluated using the Kaplan-Meier method, and differences between survival curves were compared using the log-rank test.

Immunoblotting

Immunoblotting was performed using cell lysates in RIPA buffer as described.[4] Anti-p44/42 ERK (Cell Signaling Technologies), anti–phospho-p44/42 ERK (Cell Signaling Technologies), anti-C/EBPα (Santa Cruz Biotechnology), anti-FLAG (Sigma-Aldrich), and anti-GAPDH (Hy Test Ltd) antibodies were used.

Results and discussion

The important role of TRIB1 on the MAPK signaling suggests that *TRIB1* alterations may occur in some AML cases, which do not show overlapping mutations in the pathway members, such as FLT3, KIT, or RAS. Therefore, we tried to search mutations of *TRIB1* in cases of ML-DS and TL in which such mutations are infrequent.[9] In a case of DS-AMKL (case 84), a nucleotide change from guanine to thymine has been identified at 902 that results in amino acid alteration from arginine 107 (R107) to leucine (Figure 1B). The sequence changes were confirmed by subcloning the PCR product into the TA-type plasmid vector (data not shown). The nucleotide change was not observed in the DNA sample derived from the nail of the same patient at all (Figure 1C), indicating that this change is a somatic mutation. Interestingly, the mutation was retained in the peripheral blood sample in the complete remission stage in which the GATA1 mutation completely disappeared (Figure 1C-D). These results indicate that the *TRIB1* mutation precedes the onset of TL and the *GATA1* mutation, and suggest that *TRIB1* mutation occurred at the hematopoietic stem cell level and that the clone retaining the *TRIB1* mutation survived after chemotherapy. In case 84, there was no mutation for *FLT3* exons 14, 15, and 20, *PTPN11* exons 3 and 13, *KRAS* exons 2, 3, and 5, and *KIT* exons 8, 11, and 17 by the high-resolution melt analysis (data not shown).

An additional mutation was found in a case of TL (case 109) at the nucleotides 805 and 806 from GC to AT, which results in amino acid conversion from alanine (A75) to isoleucine (supplemental Figure 1, available on the *Blood* Web site; see the Supplemental Materials link at the top of the online article). *TRIB1* expression in DS-related and DS-unrelated leukemias was examined by real-time quantitative RT-PCR (supplemental Figure 2).

R107 is located within a psuedokinase domain of TRIB1 that is considered as a functionally core domain of TRIB family proteins.[10] Sequence comparison among 3 TRIB family proteins as well as tribbles homologs in other organisms revealed that the R107 is well conserved in mammalian TRIB1 and TRIB2,[10] suggesting that this arginine residue is evolutionary conserved and may be related to an important function. On the other hand, A75 is located outside of the pseudokinase domain, not conserved between human and mouse, or other tribbles homologs. Moreover, the N-terminal domain containing A75 is dispensable for the leukemogenic activity of Trib1.[4] Therefore, we tried to investigate whether the R107L mutation could affect the leukemogenic activity of *TRIB1*.

R107L was introduced into the murine *Trib1* cDNA by site-directed mutagenesis. Both WT and R107L cDNAs were subcloned into the pMYs-IRES-GFP retroviral vector and were used for retrovirus-mediated gene transfer followed by bone marrow transfer according to the method previously described.[1] All the mice

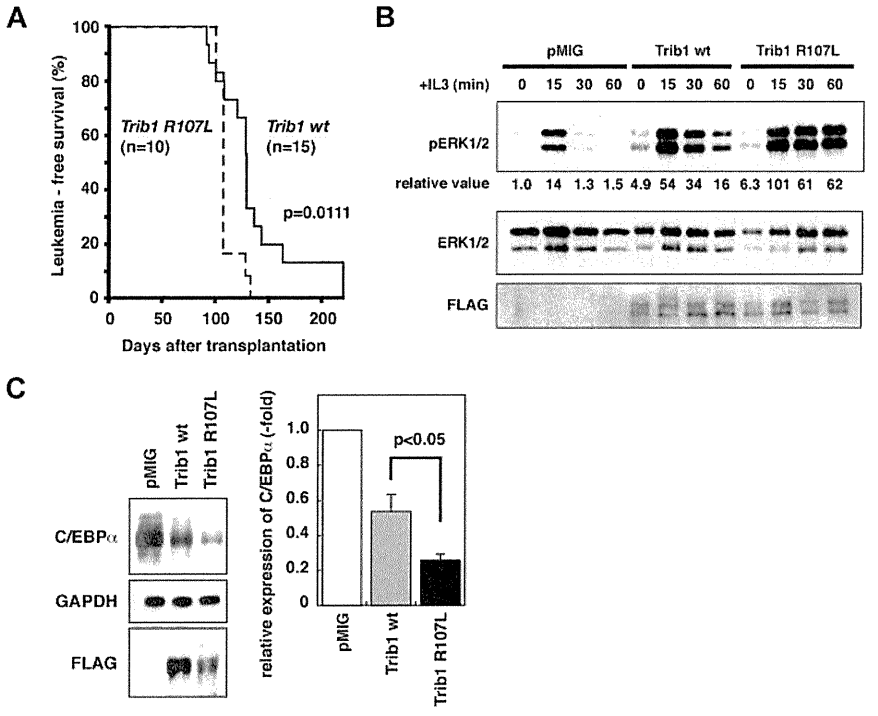

Figure 2. AML development by bone marrow transfer using *Trib1* WT and R107L. (A) Kaplan-Meier survival curves are shown. The *P* value was calculated with the log-rank test. (B) Immunoblot analysis of *Trib1* WT AML (Mac-1 56.2%, Gr-1 52.5%, $CD34^{lo}$, c-kit^{-}, Sca-1^{-}) and R107L AML (Mac-1 41.4%, Gr-1 25.2%, $Cd34^{lo}$, c-kit^{lo}, Sca-1^{-}) derived from bone marrow of recipient mice (WT #T73 and R107L #T151 in supplemental Table 1). Enhancement of ERK phosphorylation is more significant in R107L. Relative values of ERK phosphorylation were calculated by densitometric analysis. (C) Immunoblot analysis for C/EBPα of the same AML samples as in panel B. Relative expression level of C/EBPα is quantitated (right).

transplanted with bone marrow cells expressing WT (n = 15) or R107L (n = 12) developed AML (Figure 2A). The mean survival time was shorter in the recipients with R107L-expressing bone marrow cells (110 days) than those with WT (136 days; Figure 2A). The difference was significant ($P = .0111$, log-rank test). The result indicates that the R107L mutation enhances the leukemogenic activity of TRIB1. These results also suggest that *TRIB1* mutation might cooperate with *GATA1* mutation in the genesis of DS-AMKL, and that trisomy 21, *TRIB1*, and *GATA1* mutations occurred consecutively, which contributed to the multistep leukemogenic process.

We have shown that TRIB1 interacts with MEK1 and enhances phosphorylation of ERK.[2] The R107L mutant enhanced ERK phosphorylation more extensively than WT (Figure 2B) in AML cells derived from bone marrow of recipient mice, and more significant degradation of C/EBPα was induced by the R107L mutant (Figure 2C). These findings might be correlated to the enhanced leukemogenic activity of the mutant. Both R107L and WT proteins could interact with MEK1, having the binding motif in their C-termini. The residue 107 is located at subdomain II of the pseudokinase domain.[11] The mutation may affect conformation of the domain and may promote the MEK1 function on ERK, although additional studies are required to address the possibility. A recent study demonstrates that Trib1 and Trib2 failed to show ERK phosphorylation in 32D cells.[12] The different response to Trib1 between primary leukemic cells and the cell line might depend on the cellular context and/or combination of additional mutations. The AML phenotypes were somewhat varied in each case and Mac-1–positive/Gr-1–negative AMLs were more remarkable in WT than in R107L, although the difference was not statistically significant (supplemental Figures 3-4; supplemental Table 1). The current study underscores the role of TRIB1 in human leukemogenesis and the significance of the R107L mutation in its function. Further sequence analysis of tribbles family genes in a larger cohort will emphasize the importance of R107L and/or additional mutations of *TRIB1* in leukemic patients.

Acknowledgments

This work was supported by KAKENHI (Grant-in-Aid for Scientific Research) on Priority Areas Integrative Research Toward the Conquest of Cancer (E.I. and T.N.) and the Ministry of Education, Culture, Sports, Science and Technology of Japan (Young Scientists, T.Y.).

Authorship

Contribution: T.Y., E.I., Y.H., and T.N. designed and performed the research and wrote the manuscript; T. Toki, Y.A., R.K., and M.-j.P. performed the research; and Y.K., T. Takahara, and Y.Y. contributed to the bone marrow transplantation analysis.

Conflict-of-interest disclosure: The authors declare no competing financial interests.

Correspondence: Takuro Nakamura, Division of Carcinogenesis, Cancer Institute, Japanese Foundation for Cancer Research, 3-8-31 Ariake, Koto-ku, Tokyo 135-8550, Japan; e-mail: takuro-ind@umin.net.

References

1. Shimizu R, Engel JD, Yamamoto M. GATA1-related leukaemias. *Nat Rev Cancer.* 2008;8(4):279-287.
2. Jin G, Yamazaki Y, Takuwa M, et al. Trib1 and Evi1 cooperate with Hoxa and Meis1 in myeloid leukemogenesis. *Blood.* 2007;109(9):3998-4005.
3. Kiss-Toth E, Bagstaff SM, Sung HY, et al. Human Tribbles, a protein family controlling mitogen-activated protein kinase cascades. *J Biol Chem.* 2004;279(41):42703-42708.
4. Yokoyama T, Kanno Y, Yamazaki Y, et al. Trib1 links the MEK/ERK pathway in myeloid

leukemogenesis. *Blood.* 2010;116(15):2768-2775.

5. Keeshan K, He Y, Wouters BJ, et al. Tribbles homolog 2 inactivates C/EBPalpha and causes acute myelogenous leukemia. *Cancer Cell.* 2006; 10(5):401-411.
6. Storlazzi CT, Fioretos T, Surace C, et al. MYC-containing double minutes in hematologic malignancies: evidence in favor of the episome model and exclusion of MYC as the target gene. *Hum Mol Genet.* 2006;15(6):933-942.
7. Kanezaki R, Toki T, Terui K, et al. Down syndrome and GATA1 mutations in transient abnormal myeloproliferative disorder: mutation classes correlate with progression to myeloid leukemia. *Blood.* 2010;116(22):4631-4638.
8. Kogan SC, Ward JM, Anver MR, et al. Bethesda proposal for classification of nonlymphoid hematopoietic neoplasms in mice. *Blood.* 2002;100(1): 238-245.
9. Toki T, Kanezaki R, Adachi S, et al. The key role of stem cell factor/KIT signaling in the proliferation of blast cells from Down syndrome-related leukemia. *Leukemia.* 2009;23(1):95-103.
10. Hegedus Z, Czibula A, Kiss-Toth E. Tribbles: a family of kinase-like proteins with potent signaling regulatory function. *Cell Signal.* 2007;19(2):238-250.
11. Yokoyama T, Nakamura T. Tribbles in disease: signaling pathways important for cellular function and neoplastic transformation. *Cancer Sci.* 2011;102(6):1115-1122.
12. Dedhia PH, Keeshan K, Uljon S, et al. Differential ability of Tribbles family members to promote degradation of C/EBPalpha and induce acute myelogenous leukemia. *Blood.* 2010; 116(8):1321-1328.

Photochemistry and Photobiology, 2011, 87: 1138–1145

Roles of Porphyrin and Iron Metabolisms in the δ-Aminolevulinic Acid (ALA)-induced Accumulation of Protoporphyrin and Photodamage of Tumor Cells

Yoshiko Ohgari[1], Yoshinobu Miyata[1], Taeko Miyagi[1], Saki Gotoh[1], Takano Ohta[1], Takao Kataoka[1], Kazumichi Furuyama[2] and Shigeru Taketani*[1,3]

[1]Department of Biotechnology, Kyoto Institute of Technology, Kyoto, Japan
[2]Department of Molecular Biology and Applied Physiology, Tohoku University Graduate School of Medicine, Sendai, Miyagi, Japan
[3]Insect Biomedical Center, Kyoto Institute of Technology, Kyoto, Japan

Received 13 April 2011, accepted 29 May 2011, DOI: 10.1111/j.1751-1097.2011.00950.x

ABSTRACT

δ-Aminolevulinic acid (ALA)-induced porphyrin accumulation is widely used in the treatment of cancer, as photodynamic therapy. To clarify the mechanisms of the tumor-preferential accumulation of protoporphyrin, we examined the effect of the expression of heme-biosynthetic and -degradative enzymes on the ALA-induced accumulation of protoporphyrin as well as photodamage. The transient expression of heme-biosynthetic enzymes in HeLa cells caused variations of the ALA-induced accumulation of protoporphyrin. When ALA-treated cells were exposed to white light, the extent of photodamage of the cells was dependent on the accumulation of protoporphyrin. The decrease of the accumulation of protoporphyrin was observed in the cells treated with inducers of heme oxygenase (HO)-1. The ALA-dependent accumulation of protoporphyrin was decreased in HeLa cells by transfection with HO-1 and HO-2 cDNA. Conversely, knockdown of HO-1/-2 with siRNAs enhanced the ALA-induced protoporphyrin accumulation and photodamage. The ALA effect was decreased with HeLa cells expressing mitoferrin-2, a mitochondrial iron transporter, whereas it was enhanced by the mitoferrin-2 siRNA transfection. These results indicated that not only the production of porphyrin intermediates but also the reuse of iron from heme and mitochondrial iron utilization control the ALA-induced accumulation of protoporphyrin in cancerous cells.

INTRODUCTION

Photodynamic therapy (PDT) was developed as treatment of nonmelanoma skin tumors and preneoplastic skin lesions. PDT includes the activation of photosensitizer, which causes the release of singlet oxygen and other reactive oxygen species upon exposure to light, resulting in photodamage of cells, followed by tissue destruction (1). In tumor cells, *via* the heme biosynthesis pathway, photosynthesizer protoporphyrin is synthesized from a large amount of exogenous ALA and accumulates in a specific manner (2). The application of ALA following PDT treatment has been used in the treatment of skin diseases and has advantages over systemic administration in that the entire body does not face sensitization (3,4). ALA-induced PDT has been successfully applied in various medical fields, including urology, gastroenterology and dermatology (3–5). In heme biosynthesis, ALA is catalyzed by four cytosolic enzymes, ALA-dehydratase, porphobilinogen deaminase (PBGD), uroporphyrinogen synthase (UROS) and uroporphyrinogen decarboxylase and by two mitochondrial enzymes, coproporphyrinogen oxidase (CPOX) and protoporphyrinogen oxidase (PPOX), converting to protoporphyrin (6). Finally, ferrochelatase (FECH) catalyzes the insertion of ferrous ions into protoporphyrin to produce heme (7). Although there are reports that ALA-induced PDT can also be used as a fluorescence detection marker for the photodiagnosis of tumors (3,4,8), the mechanisms involved in the specific accumulation of protoporphyrin in cancerous tissues have not been clearly demonstrated. Previously, we (7,8) reported that protoporphyrin accumulates owing to limited capacity for the FECH reaction. In addition, we also reported an increase in the uptake of ALA by cancerous cells (8).

Heme oxygenase (HO) is the rate-limiting enzyme in the cellular catabolism of heme to biliverdin, carbon monoxide and free iron. Biliverdin is subsequently converted to bilirubin by biliverdin reductase (9,10). The enzyme is expressed in a variety of organisms. In mammals, two HO isoforms, HO-1 and HO-2, have been reported. The expression of HO-1 is induced by heme, a substrate of the enzyme and metal ions, such as arsenite and cadmium, whereas that of HO-2 is constant (10). Interestingly, most of the known HO-1 inducers stimulate the production of ROS or lead to a depletion of glutathione levels, indicating the involvement of the induction of HO-1 in cellular protection against oxidative stress (11,12). The induced HO-1 could have an advantage in cell growth, resulting in a protective effect against the photosensitivity of tumors, whereas the knockdown of HO-1 gives rise to suppression of cell growth with failure in the photosensitivity (13). In contrast, the reduced expression of HO-1 mRNA by siRNA increased cell death upon ALA-PDT (14). Thus, the effect of the expression of HO-1 on ALA-PDT is inconclusive. Furthermore, the contribution of HO-2 to the effectiveness of ALA-PDT is unclear.

*Corresponding author email: taketani@kit.ac.jp (Shigeru Taketani)

Iron utilization in mitochondria in cancerous cells also remains poorly understood. It was shown that functions of the respiratory chain enzymes including iron- or heme-containing proteins were impaired in tumors (15). As for mitochondrial iron metabolism, mitoferrin, a mitochondrial iron importer, transports iron in mitochondria and can regulate iron-chelation into protoporphyrin by FECH (16). Mitoferrin-1 is synthesized in erythroid cells, whereas mitoferrin-2 is synthesized in various tissues (16). Otherwise, iron delivery to the iron-sulfur cluster biosynthetic machinery can be mediated by frataxin, a mitochondrial iron-chaperon (17). The reduction of the expression of frataxin causes Friedreich's ataxia, an inherited neurodegenerative disorder (17). Targeted disruption of frataxin in murine hepatocytes causes decreased life span and increased liver tumor formation, whereas the over expression of frataxin leads to inhibition of cell growth of cancer, by increasing oxidative phosphorylation (18). Thus, iron deficiency related to FECH in cancerous cells may be responsible for the ALA-induced accumulation of protoporphyrin. Previous studies (8,19) also showed that removal of iron from the cells with an iron chelator, desferrioxamine, markedly enhanced the ALA-induced accumulation of protoporphyrin. However, as desferrioxamine has a protective effect against phototoxicity *in vitro* and *in vivo*, it did not appear to confer additional benefit in ALA-PDT (20). Therefore, it is necessary to clarify the utilization of mitochondrial iron for heme production. In this study, we investigated the role of the utilization of iron and the recycling of iron from heme for the ALA-induced accumulation of protoporphyrin and photodamage. Down-regulation of the expression of iron-metabolizing molecules mitoferrin-2, frataxin and HO-1/-2 increased the ALA-induced photodamage, whereas up-regulated expression gave the reverse effect. The importance of increased expression of porphyrin-metabolizing enzymes on ALA-PDT was also shown.

MATERIALS AND METHODS

Materials. Protoporphyrin IX, cobalt-protoporphyrin (Co-PP) and tin-protoporphyrin (Sn-PP) were purchased from Frontier Scientific Co. (Logan, UT). The antibodies for HO-1, HO-2 and actin used were as previously described (10). Monoclonal antibodies for frataxin and HA were products of Millipore Co. (Billerica, MA) and MBL Laboratories (Tokyo, Japan), respectively. HO-1 (No. sc-44306), frataxin (No. sc-40580), mitoferrin-2 (No. sc-90800) and control siRNAs (No. sc-37007) were products of Santa Cruz Biotechnology (Santa Cruz, CA). HO-2 siRNA was synthesized by Sigma–Aldrich (Tokyo, Japan): sense r(CCACCACGGCACUUUACUUCA) and antisense r(AAGUAAAGUGCCGUGGUGGCC). All other chemicals used were of analytical grade.

Plasmids. Plasmids pcDNA3-HF (human FECH) (8), pcDNA3-HCPOX (human CPOX) (21), pCD-PPOX (human PPOX) (22), pCAG-HMBSu (human nonerythroid PBGD) (23) and pCAG-UROS (human nonerythroid UROS) (23) were used for the expression of enzymes in cells. Plasmids pHHO-1 and pHHO-2 carrying human HO-1 and HO-2 cDNAs, respectively, were kind gifts from Dr. Shibahara (24,25). To construct pcDNA3-frataxin, PCR was performed with mouse liver cDNA library. Primers 5′-AAGGATCCATGTGGACT CTCGGGCGC-3′ and 5′-AAGGATCCTCAAGCATCTTTTCCGG A-3′ were used. Amplified cDNAs were digested with *Bam*HI and ligated into *Bam*HI-digested pcDNA3. To obtain the full-length cDNA fragment of human mitoferrin-2, PCR reaction was performed with the following primers: 5′-AATCTAGAGAGTTGGAGGG GCGGGGT-3 and 5′-AAAAGCTTGCCAGCCCTCCACTCT-3′ for mitoferrin-2 and human kidney cDNA library as a template. Then, to make mammalian expression vector carrying mitoferrin-2 containing an HA-tag at the C-terminus, the amplified cDNA was ligated into the *Xba*I/*Hind*III site of the vector pCG-C-HA (26).

Cell cultures. Human epithelial cervical cancer HeLa cells were grown in Dulbecco's modified Eagle's medium (DMEM) supplemented with fetal calf serum (FCS) and antibiotics. The cells (1×10^5) in a 1.5-cm-diameter dish were transfected using Lipofectamine 2000 (Invitrogen Co., San Jose, CA) with the indicated plasmid then incubated in the presence of 10% FCS at 37°C for 16–24 h (26). The cells also transfected with siRNAs were cultured for 48 h. The cells were then incubated in the absence or presence of ALA (0.5–1 mM) for 16 h before being exposed to light, as described previously (7,8).

Exposure of the cells to light. The cells were incubated with ALA (1 mM) for 8–16 h and 1.0 mL of fresh drug-free medium was then added. Irradiation with visible light was carried out under sterile conditions, using a fluorescence lamp, in a CO_2 incubator, as described previously (8,27). Cell viability was measured by 3-(4,5-dimethylthiazol-2-yl)-2,5-diphenyl-2H-tetrazolium bromide (MTT) assay. Each experiment was carried out in triplicate or quadruplicate. Cell viability (cell survival) is expressed as a percentage of control cells. Porphyrins were extracted from the cells with 96% ethanol containing 0.5 M HCl (8). The amount of protoporphyrin was determined by fluorescence spectrophotometry, as previously described (8,27).

Immunoblotting. The lysates from HeLa cells were subjected to sodium dodecylsulfate-polyacrylamide gel electrophoresis (SDS-PAGE) and electroblotted onto poly(vinylidene difluoride) (PVDF) membrane (Bio-Rad Laboratories, Hercules, CA). Immunoblotting was carried out with antibodies for HO-1, HO-2, HA, frataxin and actin, as the primary antibodies (8).

Reverse transcriptase (RT)-PCR analysis. Total RNA was isolated from the cells by the guanidium isothiocyanate method (26). Single-strand cDNA derived from the RNA was synthesized with the oligo (dT) primer, using ReveTra Ace (Toyobo, Co., Tokyo, Japan), followed by PCR, using the indicated primers. The amount of cDNA added to the reaction mixture was normalized by the intensity of glyceraldehyde-3-phosphate dehydrogenase (GAPDH) amplicon. The cDNAs obtained were analyzed using a 1% agarose gel and electrophoresed. The primers were 5′-CCGGGGCCGGGGGACCTTAG-3′ (forward) and 5′-GCGGGTACCCACGCGAATCAC-3′ for PBGD, 5′-CCCCATCGGAAATTGCTTAGG-3′ (forward) and 5′-CTTTCC CAGACTTCAGTTTTATTG-3′ for UROS, 5′-ATGTTGCCTAAGA GACCTC-3′ (forward) and 5′-ACAAAATGGCAATTTACC-3′ for CPOX, 5′-CCCACAGCCAGACTCAGC-3′ (forward) and 5′-GCTG TTAGGTTCTGTGCC-3′ for PPOX, 5′-GTGCAAAACCTCAAG TT-3′ (forward) and 5′-TCACAGCTCCTGGCTGGT-3′ for FECH, 5′-ATGTGGACTCTCGGGCGC-3′ (forward) and 5′-CTCAAGCA TCTTTTCCGGA-3′ for frataxin, 5′-GAGTTGGAGGGGCGGG GT-3′ (forward) and 5′-GCCAGCCCTCCACTCT-3′ for mitoferrin-2 and 5′-TGGGTGTGAACCACGAGA-3′ (forward) and 5′-TTACT CCTTGGAGGCCATG-3′ for GAPDH.

RESULTS

Effect of the expression of porphyrin-biosynthetic enzymes on the ALA-induced accumulation of protoporphyrin and photodamage in HeLa cells

Previously, we (8) reported that the decrease of the expression of FECH led to enhancement of the ALA-induced accumulation and photodamage. To examine whether other heme-biosynthetic enzymes are involved in the enhancement of ALA-induced accumulation of protoporphyrin, HeLa cells were transfected with pcDNA3-HF, pcDNA3-HCPOX, pCD-PPOX, pCAG-HMBSu and pCAG-UROS. The expression of these enzymes was not examined owing to lack of availability of the corresponding antibody, but RT-PCR analysis showed the increased expression of the corresponding transcript by transfection (Fig. 1A). The cells were incubated with 1 mM ALA and the accumulation of protoporphyrin was examined.

As shown in Fig. 1B, the highest accumulation of protoporphyrin in PBGD-transiently expressing cells was observed

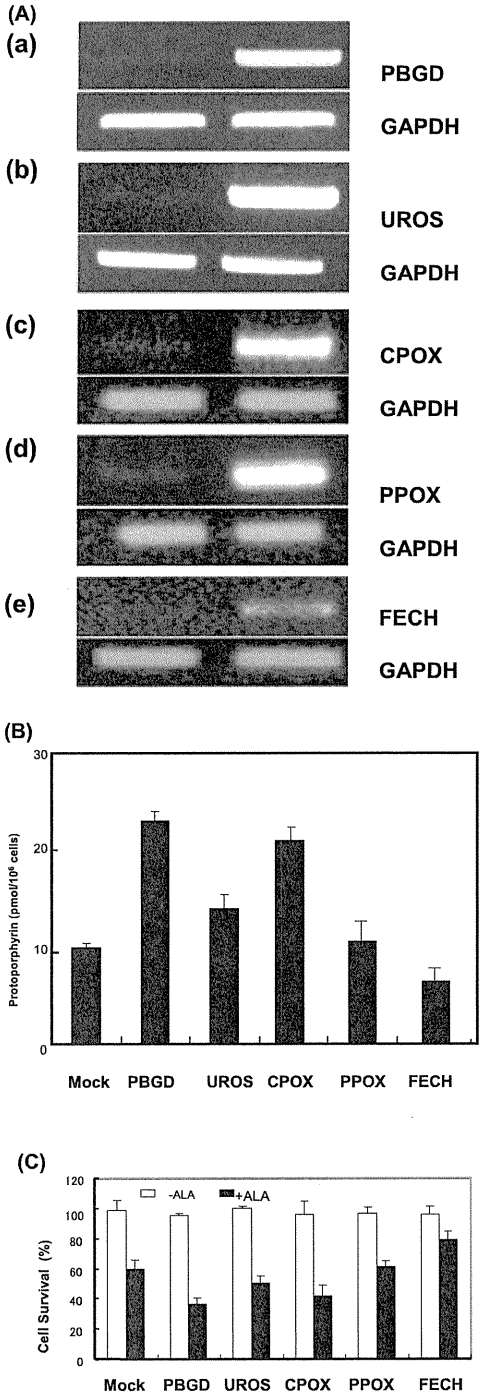

Figure 1. Effect of the expression of heme-biosynthetic enzymes on ALA-induced accumulation of protoporphyrin and photodamage in HeLa cells. (A) HeLa cells were transfected with pcDNA3-HF, pcDNA3-HCPOX, pCD-PPOX, pCAG-HMBSu and pCAG-UROS. After 16-h incubation, RNA was isolated and treated with DNase I. RT-PCR for PBGD (a), UROS (b), CPOX (c), PPOX (d) and FECH mRNA (e) was performed; (B) Effect of the expression of PBGD, UROS, CPOX, PPOX and FECH on the ALA-induced accumulation of protoporphyrin. HeLa cells (5×10^5) transfected with the indicated plasmids were incubated for 24 h and treated with 1 mM ALA for 16 h. The cells were washed twice with phosphate-buffered saline, then porphyrin was extracted and measured fluorospectrophotometrically; (C) Photosensitivity. Fresh DMEM was added to the cells treated as above, followed by exposure to white light; then surviving cells were assessed by MTT assay. Data are the mean ± SD of three independent experiments.

compared with that in control cells. The expression of UROS or CPOX also increased the accumulation. The accumulation in FECH-expressing cells was decreased, whereas that in PPOX-expressing cells was similar to that in the control. When enzyme-expressing cells were exposed to white light and photodamage was examined, the extent of cell survival was found to be related to low accumulation of protoporphyrin (Fig. 1C). No significant cell death was observed by irradiation minus ALA or by treatment with ALA minus light (data not shown). These results indicated that increase in the expression of heme-biosynthetic enzymes, including PBGD, UROS and CPOX led to high accumulation of protoporphyrin.

Involvement of iron reutilization from heme in ALA-induced accumulation of protoporphyrin and photodamage in HeLa cells

To examine if iron-containing compounds decrease the accumulation of protoporphyrin from ALA, HeLa cells were incubated with 0.5 mM ALA by the addition of 10 μM hemin or 50 μM Fe-NTA for 16 h. Porphyrins were extracted from the cells and determined. As shown in Fig. 2A, the

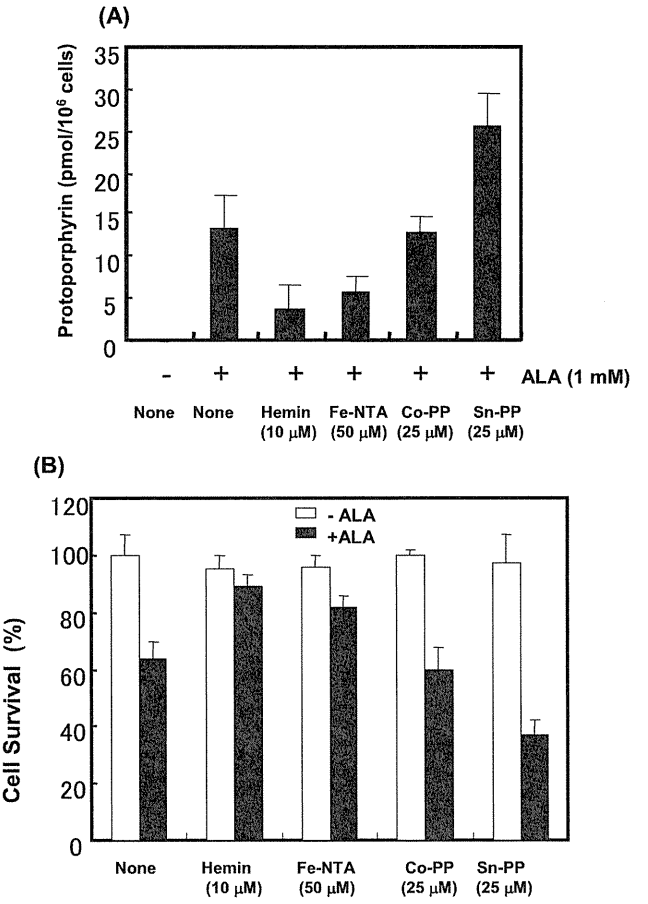

Figure 2. Effect of metalloporphyrins and Fe-NTA on ALA-induced accumulation of protoporphyrin and photodamage. (A) Effect of hemin, Fe-NTA, Co-PP and Sn-PP on the ALA-induced accumulation of protoporphyrin. HeLa cells (5×10^5) were incubated with 1 mM ALA plus the indicated concentration of chemicals for 16 h. Porphyrin was extracted from the cells and measured using a fluorospectrophotometer; (B) Effect of hemin, Fe-NTA, Co-PP and Sn-PP on ALA-induced photodamage. The cells treated as above were irradiated, and survival of the cells was analyzed by MTT assay. Data are the mean ± SD of three to four independent experiments.

accumulation of ALA-induced protoporphyrin in hemin- or ferric ion-nitrilotriacetate (FeNTA)-treated cells was decreased, compared with that in ALA-treated cells. Sn-PP, an inhibitor of HO, increased the accumulation of protoporphyrin. Co-PP, a substrate of HO, was without effect on the accumulation. When the ALA-induced photodamage was examined, hemin and Fe-NTA reduced the photodamage dependent on the decrease of protoporphyrin (Fig. 2B). Sn-PP but not Co-PP increased the photodamage. The above results suggest that the generation of iron from heme may decrease the photodamage and accumulation of protoporphyrin.

Our previous studies (28,29) showed that treatment of the cells with hemin and metal ions resulted in the induction of HO-1. When the cells were treated with hemin, arsenite or cadmium ions for 16 h, HO-1 was markedly induced (Fig. 3A). The ALA-induced accumulation of protoporphyrin in arsenite and cadmium ion-treated cells was decreased compared with that in the control, but the extent was less than that in the case of hemin (Fig. 3A). These results suggest that reutilization of iron generated from heme by HO led to the decrease of the accumulation of protoporphyrin. Then, the HeLa cells were transfected with pHHO-1 or pHHO-2. As shown in Fig. 3B, the expression of HO-1 and HO-2 by the transfection was increased. When the cells were then treated with ALA, the accumulation of protoporphyrin in HO-1 or HO-2-expressing cells was decreased, indicating that the increase in the expression of HOs can facilitate the recycling of iron from heme. These observations led us to examine if knockdown of the HO-1/-2 expression affects the accumulation of protoporphyrin. When HeLa cells were transfected with HO-1/-2 siRNAs and incubated for 48 h, the levels of HO-1 and HO-2 proteins were markedly decreased (Fig. 4A). After the subsequent 16-h incubation with ALA, the content of porphyrin was measured. As expected, the accumulation of protoporphyrin was increased by knockdown of HO-1 and HO-2 (Fig. 4B). The photodamage by HO-1/-2 double knockdown was much greater than that by transfection of control RNA (Fig. 4C). These results indicate that cessation of the recycling of iron from heme enhances the ALA-induced photodamage.

Involvement of mitochondrial iron-metabolizing proteins in regulating the ALA-induced accumulation of protoporphyrin and photodamage

Recently, some researchers (16) reported that mitochondrial iron-metabolizing proteins including mitoferrin-2 and frataxin regulate heme and Fe-S cluster biosynthesis. To clarify the involvement of these proteins in the ALA-induced accumulation of protoporphyrin, HeLa cells transiently expressing frataxin or nonerythroid type mitoferrin-2 were made (Fig. 5A). After these cells were incubated with ALA for 16 h, porphyrin in the cells was examined. The expression of mitoferrin-2, but not frataxin, decreased the ALA-induced accumulation of protoporphyrin in a dose-dependent manner (Fig. 5B). The ALA-induced photodamage with these cells was also examined. The light-resistant cells were increased dependent on the decrease of protoporphyrin (Fig. 5C). Finally, knockdown of the expression of frataxin and mitoferrin-2 using siRNA was carried out (Fig. 6A). The ALA-induced accumulation of protoporphyrin in frataxin- or mitoferrin-2-deficient cells was more than that of control cells (Fig. 6B). Upon exposure of the cells to light, photodamage of frataxin- or mitoferrin-2-deficient cells was greater than that of the

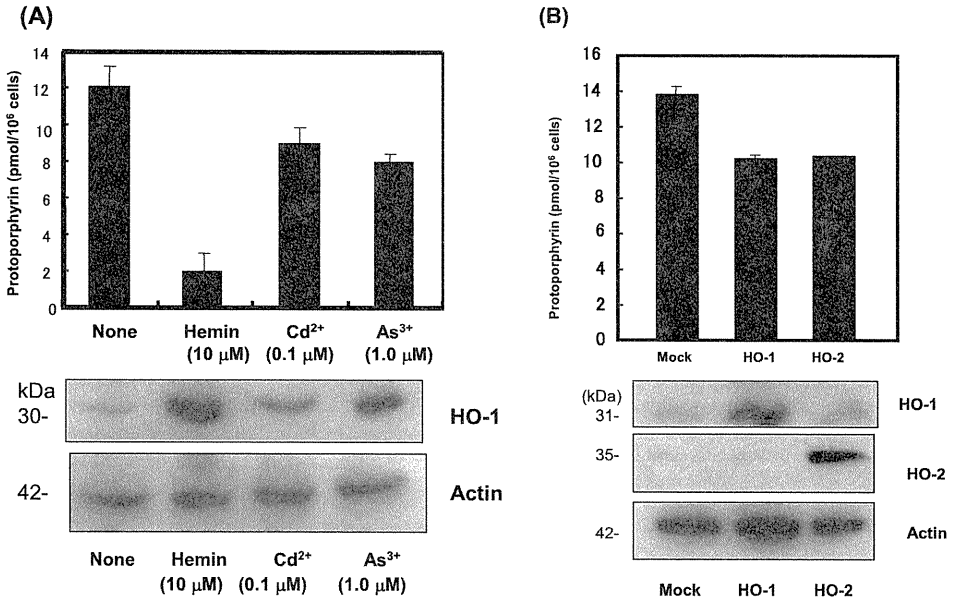

Figure 3. Reduction of ALA-induced accumulation of protoporphyrin and photodamage by the expression of HO-1,-2. (A) Effect of hemin, sodium arsenite and cadmium chloride on the ALA-dependent accumulation of protoporphyrin. Upper panel: HeLa cells (5×10^5) were treated with the above chemicals at the indicated concentration plus 1 mM ALA for 16 h. The accumulated protoporphyrin was measured. Data are the mean ± SD of three independent experiments. Lower panels: Immunoblots of HO-1. Cell lysates from cells treated with hemin, sodium arsenite and cadmium chloride for 16 h were analyzed by SDS-PAGE, followed by immunoblotting; (B) Effect of over expression of HO-1 and HO-2 on the accumulation of protoporphyrin. The cells transfected with pHHO-1 and pHHO-2 were cultured for 16 h, followed by incubation with 1 mM ALA for 8 h. Upper panel: Porphyrin was extracted and determined. Lower panel: Immunoblots of HO-1 and HO-2.